SUPPLEMENTARY MATERIAL

Surface and Subsurface Radar Equations for Radar Sounders

Mark S. HAYNES

Jet Propulsion Laboratory, California Institute of Technology, Pasadena, CA, USA
Correspondence: Mark Haynes <mark.s.haynes@jpl.nasa.gov>

S1. SURFACE RADAR EQUATIONS

This section contains derivations of radar equations for normal incidence surface targets. Subsurface geometries are covered in Section S2.

S1.1. Basic Radar Equation

The radar equation is (Ulaby and others, 1982, 2014)

$$P_r = \frac{P_t G_t G_r \lambda^2 \sigma}{(4\pi)^3 R^4} \tag{S.1}$$

where P_r is the received power, P_t is the transmit power, G_t and G_r are the transmit and receive antenna gains respectively, R is the distance to the target, λ is the wavelength, and σ is the radar cross section.

If the surface is characterized by the normalized radar cross section, $\sigma = \sigma_o A$, where σ_o is independent of area, A, then the radar equation is, as usual,

$$P_r = \frac{P_t G_t G_r \lambda^2 \sigma_o A}{(4\pi)^3 R^4} \tag{S.2}$$

Derivation

The power density of the signal from the transmitter is

$$S_t = \frac{P_t G_t}{4\pi R^2} \tag{S.3}$$

The power intercepted by the target is $P_i = S_t \sigma$. This is power reradiated from the target with power density

$$S_r = \frac{P_i}{4\pi R^2} \tag{S.4}$$

The power intercepted by the receive antenna is

$$P_r = S_r A_r \tag{S.5}$$

where A_r is the effective aperture of the receive antenna.

$$A_r = \frac{G_r \lambda^2}{4\pi} \tag{S.6}$$

Putting these together gives (S.1).

S1.2. Image Method

This is the classic derivation for the radar equation over an infinite mirror, (Ulaby and others, 2014; Nguyen and Park, 2016). Assume the surface is flat and infinite with perfect reflection at normal incidence. The surface is replaced with a transmitter at distance $R = 2h$ from the receiver, Figure S1. The power density at the receiver due to the image source is

$$S_r = \frac{P_t G_t}{4\pi (2h)^2} \tag{S.7}$$

The power received is then

$$P_r = S_r A_r = S_r \frac{G_r \lambda^2}{4\pi} \tag{S.8}$$

where A_r is the effective aperture of the receiver. After including a factor of reflectivity, Γ, the radar equation derived for a flat surface under the image method is

$$P_r = \frac{P_t G_t G_r \Gamma \lambda^2}{(4\pi)^2 (2h)^2} \tag{S.9}$$

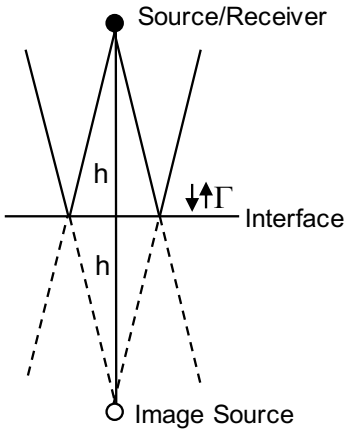

Fig. S1: Geometry of classic image approach for infinite mirror.

A similar form of this also appears in (Moore and Williams, 1957; Edison and others, 1960; Fung and Eom, 1983). This radar equation should be used to compute raw received power when the surface is considered smooth, flat, and infinite. This equation is useful when considering flat surfaces for

radiometric calibration, such as flat surface ice (e.g., non-crevassed terrestrial ice or Mars) or open water (e.g., airborne sounders). Note, the power predicted by (S.9) will match the peak power obtained in range-compressed echo simulations of perfectly flat surfaces that have been modeled with discrete sub-wavelength facets.

Equation (S.9) will predict a received power approximately 4 times less (-6 dB) than that for spherical wave incidence over a flat Frensel zone, Section S1.4, (S.28), and approximately 10 times less (-10 dB) than that derived under the 'antenna' approach, Section S1.6, (S.60). This implies that scattering beyond the Fresnel zone contributes incoherently as captured in this model. In other words, this equation will give a conservative estimate of received power in radar link budgets compared to other target areas. Equation (S.9) can also be obtained by the plane wave or 'antenna' approach, Section S1.6, if the target area is a square with side length equal to the Fresnel zone radius. In addition, (S.9) is equivalent to the radar equation derived using the subsurface image method evaluated at the surface, see (Peters and others, 2005) and Section S2.1.

S1.3. Target Backscatter

The following derivations consider the radar equation for specific target geometries. For these, the backscatter of a smooth surface under the Kirchhoff approximation, (Haynes and others, 2018; Kong, 1986; Tsang and others, 2000), is

$$\sigma_{disk} = \Gamma \frac{4\pi |I|^2}{\lambda^2} \tag{S.10}$$

where Γ is the reflectivity, $|I|^2$ is the magnitude squared of the surface phase integral for spherical incident waves. In addition, the electric field polarization is assumed constant over the surface.

For plane waves and normal incidence, the magnitude squared of the surface phase integral reduces to the target area squared (Levine, 1984):

$$\sigma_{disk} = \Gamma \frac{4\pi A^2}{\lambda^2} \tag{S.11}$$

S1.4. Fresnel Zone - Spherical Waves - Flat Surface

Here we derive the radar equation for a Fresnel zone target with spherical incidence waves over a flat surface. To do this, we compute the integral of the two-way phase over a disk out to radius a, Figure S2:

$$I = \int e^{i2kr} dS \tag{S.12}$$

$$= \int_0^{2\pi} \int_0^a e^{i2k\sqrt{h^2+\rho^2}} \rho d\rho d\theta \tag{S.13}$$

where h is the height or altitude of the sensor and $k = 2\pi/\lambda$ is the wave number. The integral is equal to

$$I = 2\pi \left. \frac{e^{2ik\sqrt{h^2+x^2}} \left(1 - 2ik\sqrt{h^2+x^2}\right)}{4k^2} \right|_0^a \tag{S.14}$$

$$= \frac{2\pi}{4k^2} \left(e^{2ik\sqrt{h^2+a^2}} \left(1 - 2ik\sqrt{h^2+a^2}\right) - e^{2ikh} \left(1 - 2ikh\right) \right) \tag{S.15}$$

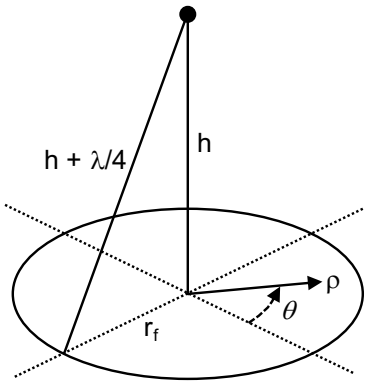

Fig. S2: Geometry for the Fresnel zone with spherical waves and flat interface.

When $h \gg a$ this can be approximated

$$I \approx \frac{2\pi}{4k^2} e^{2ikh} \left(1 - 2ikh\right) \left(e^{2ik\sqrt{h^2+a^2} - 2ikh} - 1 \right) \tag{S.16}$$

The magnitude of the integral, $|I|$, is maximized when

$$e^{2ik\sqrt{h^2+a^2} - 2ikh} = -1 \tag{S.17}$$

or

$$2k\sqrt{h^2+a^2} - 2kh = \pi m \qquad m \text{ odd} \tag{S.18}$$

Solving for a gives the radius of each Fresnel zone

$$a_m = \sqrt{\left(h + \frac{\lambda m}{4}\right)^2 - h^2} \tag{S.19}$$

The first Fresnel zone occurs when $m = 1$, or

$$r_f = \sqrt{\left(h + \frac{\lambda}{4}\right)^2 - h^2} \tag{S.20}$$

This radius corresponds to slant range from the radar that is $\lambda/4$ longer than the slant range to the nadir point and corresponds to a 2-way relative phase difference of 180 degrees between nadir and the edge of Fresnel zone. When $h \gg \lambda$, this is expanded and approximated as

$$r_f \approx \sqrt{\frac{\lambda h}{2}} \tag{S.21}$$

which appears in many places in the form of radius or diameter (Seu and others, 2007; Bruzzone and others, 2011; Schroeder and others, 2016; Haynes and others, 2018).

The magnitude squared of the phase integral is

$$|I|^2 = \frac{(2\pi)^2}{(4k^2)^2} |1 - 2ikh|^2 \left| \left(e^{2ik\sqrt{h^2+a^2} - 2ikh} - 1 \right) \right|^2 \tag{S.22}$$

$$= \frac{(2\pi)^2}{(4k^2)^2} (1 + (2kh)^2) \left(2 - 2\cos\left(2k\sqrt{h^2+a^2} - 2kh \right) \right) \tag{S.23}$$

$$\approx \frac{(2\pi)^2}{(4k^2)^2} (2kh)^2 \left(2 - 2\cos\left(2k\frac{a^2}{2h} \right) \right) \tag{S.24}$$

$$= \frac{2\pi^2}{k^2} h^2 \left(1 - \cos\left(k\frac{a^2}{h} \right) \right) \tag{S.25}$$

When the size of the disk is larger than the Fresnel zone, the value of (S.25) will oscillate between its peak and zero. This is plotted in Figure S3.

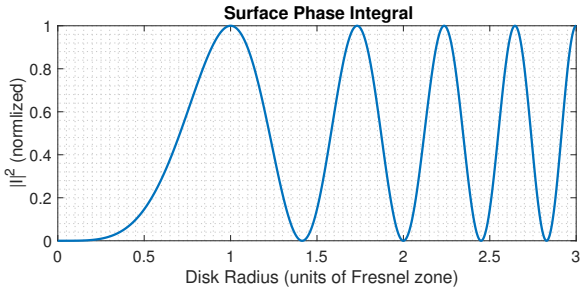

Fig. S3: Surface phase integral over a flat surface normalized magnitude squared plotted as a function of Fresnel zone radius.

Evaluated at the fresnel zone radius $a = r_f$ gives

$$|I|^2 = \frac{4\pi^2}{k^2}h^2 \tag{S.26}$$

Using (S.26) in (S.10), the backscatter of the disk is

$$\sigma_{disk}(a = r_f) = \Gamma 4\pi h^2 \tag{S.27}$$

Finally, substituting this into (S.1), the radar equation for the Fresnel zone area and spherical incident waves over a flat interface is

$$P_r = \frac{P_t G_t G_r \lambda^2 \Gamma}{(4\pi)^2 h^2} \tag{S.28}$$

This appears in (Haynes and others, 2018). The received power can be less than (S.28) if the target is bigger or smaller than exactly the Fresnel zone. To demonstrate this, we retain the oscillating component of (S.25) in (S.10), then the radar equation is instead

$$P_r = \frac{P_t G_t G_r \lambda^2 \Gamma}{2^5 \pi^2 h^2}\left(1 - \cos\left(k\frac{a^2}{h}\right)\right) \tag{S.29}$$

$$= \frac{P_t G_t G_r \Gamma}{2^5 \pi^2} F \tag{S.30}$$

$$F = \frac{1}{h_\lambda^2}\left(1 - \cos\left(2\pi\frac{a_\lambda^2}{h_\lambda}\right)\right) \tag{S.31}$$

where F is the geometric factor written in terms of disk radius and altitude in units of wavelength. Equation (S.31) is plotted in Figure S4. For a given altitude, the power is maximum at the discrete Fresnel zones. While the value can theoretically be zero, this is never encountered in practical systems. This is because a) surface targets are not perfectly isolated disks, whether physically or after SAR focusing, b) the range sampling of the time-domain response would need to be such that the surface phase integral evaluated to exactly zero, and c) the radar system would need to be truly monochromatic, rather than a pulsed or chirped radar.

In general, (S.28) is useful when considering the reflected power from a target that is exactly equal to the Fresnel zone, for example, after unfocused SAR processing. However, the interplay of along-track SAR resolution and flat surface scattering is more complicated, as discussed in (Peters and others, 2005), and so (S.28) should be considered carefully in context.

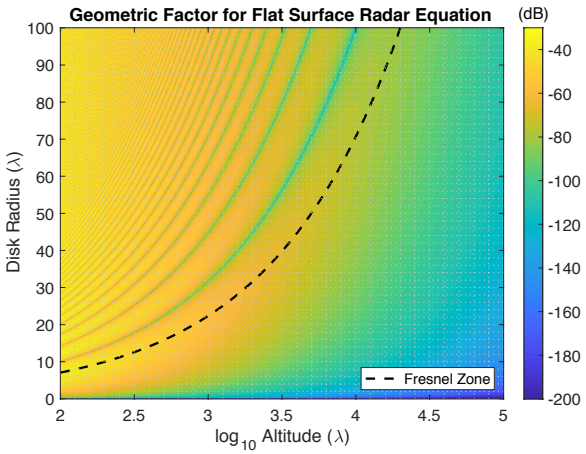

Fig. S4: Geometric factor of the radar equation for flat surface and spherical waves with normal incidence, (S.31).

S1.5. Fresnel Zone - Spherical Waves - Spherical Surface

Here we derive the Fresnel zone and radar equation for spherical waves incident on a spherical surface. The geometry is given in Figure S5. Assume the sensor is aligned on the z-axis. The surface phase integral over a spherical surface is

$$I = \int_0^{2\pi}\int_0^{\beta} e^{i2kd(\theta,\phi)} r^2 \sin\theta d\theta d\phi \tag{S.32}$$

$$d = |\mathbf{s} - \mathbf{x}| \tag{S.33}$$

$$\mathbf{s} = (r + h)\hat{z} \tag{S.34}$$

$$\mathbf{x} = r\hat{r} \tag{S.35}$$

$$= r(\sin\theta\cos\phi\hat{x} + \sin\theta\sin\phi\hat{y} + \cos\theta\hat{z}) \tag{S.36}$$

where r is the radius of the sphere, $\mathbf{s}$ is the vector of the source along the z-axis, $\mathbf{x}$ is the integration point on the sphere, θ is the polar angle between the z-axis (source direction) and the integration point, β is the integration limit of θ, ϕ is the azimuth angle in spherical coordinates, and d is the distance from the source to the integration point. Computing d^2 directly or equivalently from the law of cosines

$$d^2 = r^2 + (r + h)^2 - 2r(r + h)\cos\theta \tag{S.37}$$

Substituting (S.37) into (S.32) and evaluating the ϕ integral

$$I = 2\pi\int_0^{\beta} e^{i2k\sqrt{r^2+(r+h)^2-2r(r+h)\cos\theta}} r^2 \sin\theta d\theta \tag{S.38}$$

Approximating the square root for $\theta \ll 1$

$$\sqrt{r^2 + (r+h)^2 - 2r(r+h)\cos\theta} \approx h + \frac{(hr+r^2)}{2h}\theta^2 \tag{S.39}$$

and doing the same for $\sin\theta \approx \theta$, the surface integral becomes

$$I \approx 2\pi \int_0^\beta e^{i2k(h+\frac{(hr+r^2)}{2h}\theta^2)} r^2 \theta d\theta \tag{S.40}$$

which is evaluated as

$$I = -\frac{2\pi r^2 i e^{2ikh}(-1+e^{2i\beta^2 Bk})}{4Bk} \tag{S.41}$$

$$B = \frac{(hr+r^2)}{2h} \tag{S.42}$$

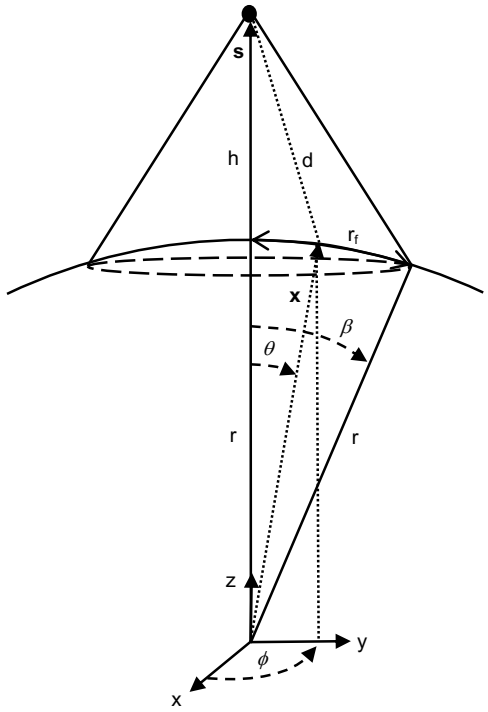

Fig. S5: Geometry for the Fresnel zone and surface phase integral for a spherical incidence waves and spherical surface.

The magnitude of the phase integral is

$$|I| = \frac{2\pi r^2 \left|-1+e^{2i\beta^2 Bk}\right|}{4Bk} \tag{S.43}$$

This is maximum when

$$2\beta^2 Bk = \pi \tag{S.44}$$

or

$$\beta^2 = \frac{\lambda h}{2(hr+r^2)} \tag{S.45}$$

The Fresnel zone radius is taken as the arc length along the surface from the z-axis to β, as $r_f = r\beta$, or

$$r_f = \sqrt{\frac{\lambda h r}{2(h+r)}} \tag{S.46}$$

This is the result in (Haynes and others, 2018), which was derived in two different ways from the geometry rather than the surface integral. The magnitude squared of the surface phase integral is

$$|I|^2 = \frac{(2\pi)^2 r^4}{(4Bk)^2}\left|-1+e^{2i\beta^2 Bk}\right|^2 \tag{S.47}$$

$$= \frac{(2\pi)^2 r^4}{(4Bk)^2} 2\left(1-\cos\left(2\beta^2 Bk\right)\right) \tag{S.48}$$

$$= \frac{(2\pi)^2 r^4}{(4k)^2}\frac{(2h)^2}{(hr+r^2)^2} 2\left(1-\cos\left(2\beta^2\frac{(hr+r^2)}{2h}k\right)\right) \tag{S.49}$$

$$= \frac{2\pi^2}{k^2}\frac{h^2 r^2}{(h+r)^2}\left(1-\cos\left(\beta^2\frac{(hr+r^2)}{h}k\right)\right) \tag{S.50}$$

Evaluated at the Fresnel zone angle, (S.45), this becomes

$$|I|^2 = \frac{2\pi^2}{k^2}\frac{h^2 r^2}{(h+r)^2}\left(1-\cos\left(\frac{\lambda h}{2(hr+r^2)}\frac{(hr+r^2)}{h}k\right)\right) \tag{S.51}$$

$$= \frac{4\pi^2}{k^2}\frac{h^2 r^2}{(h+r)^2} \tag{S.52}$$

Using (S.52) in (S.10), the backscatter from the spherical disk is

$$\sigma_{disk}(a=r_f) = \Gamma\frac{4\pi|I|^2}{\lambda^2} \tag{S.53}$$

$$= \Gamma\frac{4\pi}{\lambda^2}\frac{4\pi^2}{k^2}\frac{h^2 r^2}{(h+r)^2} \tag{S.54}$$

$$= \Gamma 4\pi h^2\frac{r^2}{(h+r)^2} \tag{S.55}$$

Substituting this into (S.1), the radar equation for the Fresnel zone and spherical incident waves over a spherical surface is

$$P_r = \frac{P_t G_t G_r \lambda^2 \Gamma}{(4\pi)^2 h^2}\frac{r^2}{(h+r)^2} \tag{S.56}$$

This is the same as (S.28) but with a correction factor for the spherical surface, which has the effect of reducing the received power. As with the flat surface, this assumes that the polarization, reflectivity and antenna gain are constant over the surface in the region of the Fresnel zone. In effect, only the area of the Fresnel zone is modified by the spherical surface.

The spherical surface correction can be written

$$\frac{r^2}{(h+r)^2} = \frac{1}{(z+1)^2} \tag{S.57}$$

where $z = h/r$ is the ratio of the sensor height and sphere radius. This is plotted in Figure S6.

Equation (S.56) and the spherical surface correction are most useful for the link budgets of planetary radar sounders when the altitude of operation is similar or might exceed the body radius, for example Mars, Europa, and Ganymede, (Haynes and others, 2018). In these situations, the total reflected power can decrease by several dB relative to a flat surface. In the case of potential future terrestrial orbiting radar sounders, the radius of Earth is large compared to typical remote sensing altitudes of several hundred kilometers, so that this correction is negligible.

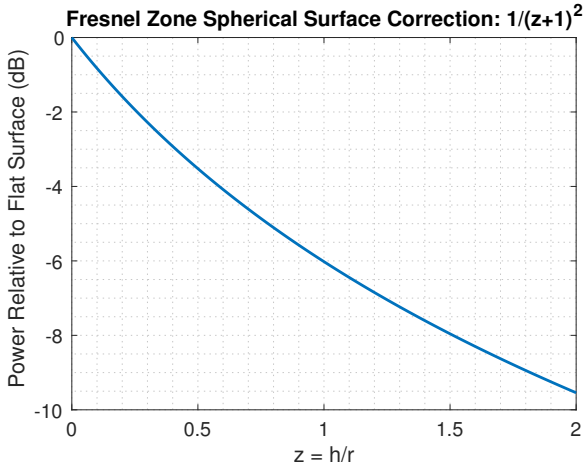

Fig. S6: Power loss of a spherical surface Fresnel zone relative to a flat surface as a function of the ratio of altitude to body radius: $z = h/r$.

S1.6. Fresnel Zone - Plane Waves or 'Antenna' Approach - Flat Surface

The 'antenna' approach is when the Fresnel disk is treated as a flat circular antenna aperture that reradiates normal incident plane waves. This is represented in Figure S7. The backscatter of the disk in this case is given by (S.11), where the area of the Fresnel zone is used as the target area.

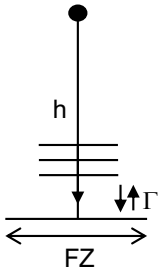

Fig. S7: Representation of the plane waves or 'antenna' approach, where the Fresnel zone is treated as an antenna aperture.

Using (S.21), the area of the Fresnel zone disk over a flat surface is

$$A = \pi r_f^2 = \frac{\pi \lambda h}{2} \tag{S.58}$$

Using this in (S.11), the backscatter is

$$\sigma_{disk} = \Gamma \pi^3 h^2 \tag{S.59}$$

Substituting this in (S.1), the radar equation for the Fresnel zone using the 'antenna' approach is equal to

$$P_r = \frac{P_t G_t G_r \lambda^2 \Gamma}{4^3 h^2} \tag{S.60}$$

This form appears in (Haynes and others, 2018). Note, if in this method the target is instead a square with side length equal to the Fresnel zone radius, then the radar equation becomes the same as that derived by the image method, (S.9). Likewise, if the target is a rectangle with along-track length equal to half the Fresnel zone radius and across-track length equal to the Fresnel zone diameter, then plane-wave incidence will again yield the image equation (S.9). The salient detail in this last case is that an along-track length equal to half a Fresnel zone radius is equal to the SAR resolution when the synthetic aperture length is equal to the Fresnel zone diameter (over a flat surface).

S2. SUBSURFACE RADAR EQUATIONS

This section contains derivations of radar equations for subsurface targets either Fresnel zone sized or arbitary. Subsurface pulse-limited geometries are covered in Section S3.

S2.1. Subsurface - Image Method - Spherical Waves - Flat Surface - Flat Subsurface

Here we derive the radar equation for a flat surface and flat subsurface interfaces using the image method, which is similar to the derivation in (Gudmandsen, 1971). The geometry is shown in Figure S8.

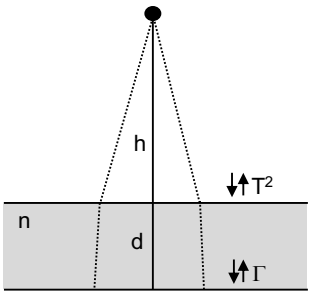

Fig. S8: Geometry for subsurface image method.

The power density of the transmitting antenna at the surface interface is

$$S = \frac{P_t G_t}{4\pi h^2} \tag{S.61}$$

where h is the sensor height above the surface. Assuming the wave impinging on the surface is planar, the total power incident on an area A is

$$P_+ = SA \tag{S.62}$$

The total power across the surface interface and just below the surface is

$$P_- = TP_+ \tag{S.63}$$

where T is the transmittivity. In order to replace the dielectric subsurface with free-space, we need to replace the source with an equivalent source in the medium that produces the same power just below the surface interface, and in a way that the refracted rays appear to emanate from this source. This source is located a height h', which will be higher than the

original source at height h. The power due to the equivalent source is given generally by

$$P' = S'A = \frac{P'_t G'_t A}{4\pi h'^2} \tag{S.64}$$

where S' is the power density of the equivalent source at the interface, and $P'_t G'_t$ is the power-gain product of the equivalent source. Equating (S.63) and (S.64), the power-gain product of the equivalent source is

$$P'_t G'_t = P_t G_t T \frac{h'^2}{h^2} \tag{S.65}$$

The dielectric can now be replaced with free-space and the original source replaced with the equivalent source which is located $h' + d$ above the subsurface interface, shown in Figure S9. Applying the image method, the power density of the image of the equivalent source, at the equivalent source, is

$$S_2 = \frac{P'_t G'_t \Gamma T}{4\pi(2(h' + d))^2} \tag{S.66}$$

where a factor of reflectivity has been included for reflection from the subsurface and a factor of transmissivity for transmission through the surface interface. The power received is then

$$P_r = S_2 A_r = \frac{S_2 G_r \lambda^2}{4\pi} \tag{S.67}$$

where G_r is the gain of the receive antenna. Putting these together, the received power is

$$P_r = \frac{P_t G_t G_r \lambda^2 T^2 \Gamma}{(4\pi)^2 (2(h' + d))^2} \frac{h'^2}{h^2} \tag{S.68}$$

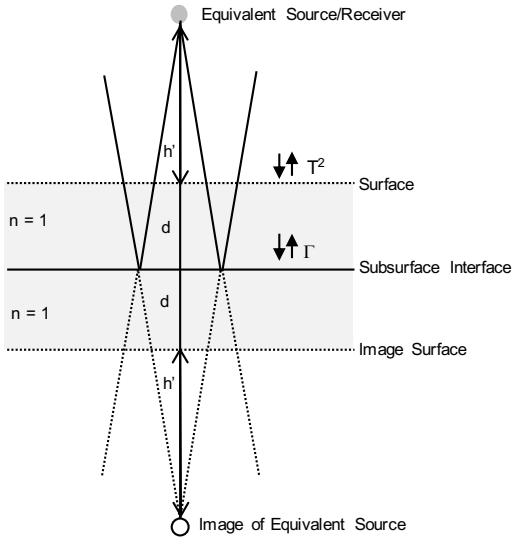

Fig. S9: In the subsurface image method, the subsurface is replaced by the image of the equivalent source/receiver in free space.

To derive the location of the equivalent source, we start with the geometry in Figure S10 and Snell's law

$$\sin\theta_i = n \sin\theta_t \tag{S.69}$$

where n is the index of refraction of the subsurface, θ_i is the incidence angle and θ_t is the transmission angle. If x is the distance along the surface from nadir to the refraction point, then $\tan\theta_i = x/h$ and $\tan\theta_t = x/h'$, where the rays of the transmitted signal intersect the equivalent source. For small angles, $\sin\theta \approx \tan\theta$, and we can approximate

$$\frac{h'}{h} = n \tag{S.70}$$

In other words, the height of the equivalent source is n times the height of the actual source. Substituting (S.70) into (S.68), the received power is

$$P_r = \frac{P_t G_t G_r \lambda^2 T^2 \Gamma}{(4\pi)^2 (2(nh + d))^2} n^2 \tag{S.71}$$

$$= \frac{P_t G_t G_r \lambda^2 T^2 \Gamma}{(4\pi)^2 (2(h + d/n))^2} \tag{S.72}$$

This is the expression (Peters and others, 2005, Eq. 1). Multiplying top and bottom by the physical distance between the source and subsurface squared, $(h + d)^2$, we get

$$P_r = \frac{P_t G_t G_r \lambda^2 T^2 \Gamma}{(4\pi)^2 (2(h + d))^2} g_r^2 \tag{S.73}$$

where g_r is the one-way refractive gain

$$g_r = \frac{h + d}{h + d/n} \tag{S.74}$$

The expression for g_r is the same as the area scaling ratio derived in (Gudmandsen, 1971). In (Gudmandsen, 1971), the total (two-way) refractive gain is given as the parameter $q = 20\log_{10}(g_r)$. We arrived at g_r^2 in (S.73), so by using $10\log_{10}$ for power these factors are equivalent. Equation (S.73) is also the same equation given in (Chyba and others, 1998), which is equivalent to that in (Peters and others, 2005), and is the same as the form in (Kofman and others, 2010) without refraction gain. The constant in the denominator, $4^3\pi^2$, is the same constant that appears in the surface radar equation for an infinite mirror. In other words, (S.73) is the infinite mirror, or image method, analog for the subsurface.

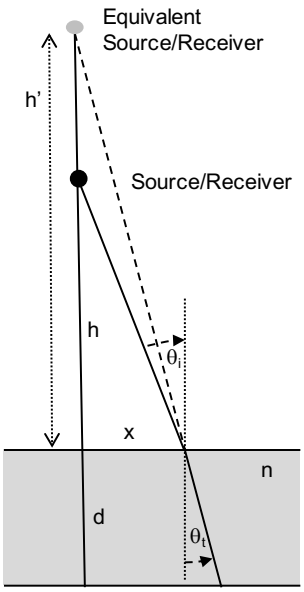

Fig. S10: Geometry for Snell's law small-angle approximation. The rays incident on the subsurface point appear to emanate from the equivalent source after the dielectric is replaced with free space.

S2.2. Refraction Gain - Flat Surface

The one-way refraction gain is again

$$g_r = \frac{h+d}{h+d/n} \tag{S.75}$$

Written in terms of the altitude to depth ratio $z = h/d$

$$g_r = \frac{z+1}{z+1/n} \tag{S.76}$$

This is plotted in Figure S11. Recall $n = \sqrt{\epsilon_r}$. For ice-like dielectrics and sensor altitudes equal to or greater than the target depth, the two-way refraction gain is generally less than 2 dB. Refraction gain decreases quickly with increasing sensor altitude. For space-borne low-frequency radar sounders, it is usually negligible. When the target is much deeper than the altitude of the sensor (e.g., when the sensor is at the surface), the two-way refraction gain approaches ϵ_r:

$$\lim_{z\to 0} g_r^2 = \epsilon_r \tag{S.77}$$

S2.3. Subsurface Nadir - General Radar Equation - Spherical Waves - Flat Surface

We derive the radar equation for an arbitrary subsurface target at nadir, represented in Figure S12. The approach is to apply power conservation by following the power through the interface to and from the target. This enables deriving a subsurface radar equation in which a Fresnel zone or other sized target can be substituted later.

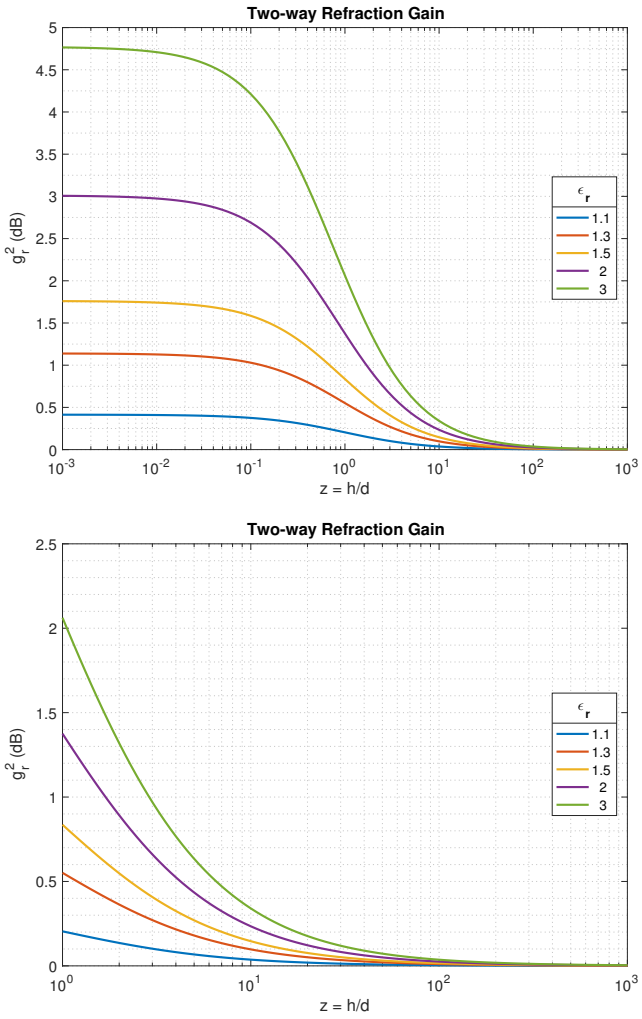

Fig. S11: Top: Two-way refractive gain as a function of altitude to depth ratio $z = h/d$. Bottom (zoom of Top): Two-way refractive gain as a function of altitude to depth ratio $z = h/d$, over a range where $h > d$.

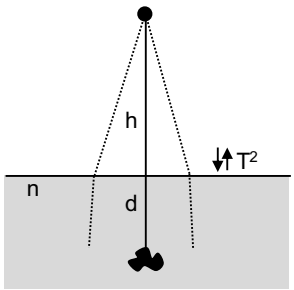

Fig. S12: Geometry for arbitrary subsurface target at nadir.

Similar to the image method, we must derive the power-gain product of an equivalent source evaluated at the interface. The steps of the derivation are identical to (S.61)-(S.65), after which the surface interface can be replaced with the equivalent source, Figure S13. In the previous image method, the subsurface was replaced with free-space. Here we replace free-space with dielectric, because the waves are

propagating with rays as though the equivalent source is in the subsurface medium. Note, geometric fall-off does not depend on the properties of the medium.

Taking the equivalent source to be in the medium, the power density of the equivalent source at range R' is

$$S' = \frac{P_t' G_t'}{4\pi R'^2} = \frac{P_t G_t T}{4\pi R'^2} \frac{h'^2}{h^2} \tag{S.78}$$

The power density radiated by the equivalent source is evaluated at the subsurface target $h' + d$

$$S_d = \frac{P_t G_t T}{4\pi (h' + d)^2} \frac{h'^2}{h^2} \tag{S.79}$$

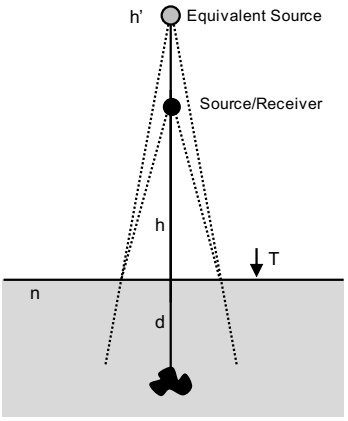

Fig. S13: Geometry for equivalent source/receiver in the medium of the subsurface.

The power scattered by the subsurface target is

$$P_\sigma = S_d \sigma_{\epsilon_r} \tag{S.80}$$

where σ_{ϵ_r} is the radar backscatter of the target in a medium with relative permittivity ϵ_r.

The power density of the field scattered by the target evaluated at the interface is

$$S_\sigma = \frac{P_\sigma}{4\pi d^2} \tag{S.81}$$

The scattered power just below the surface interface incident on an area A is

$$P_{--} = S_\sigma A \tag{S.82}$$

The power above the surface interface is

$$P_{++} = T P_{--} \tag{S.83}$$

Next, we need to replace the target with an equivalent target in order to replace the dielectric with free-space, Figure S14. The equivalent target must be positioned so that the rays radiated from the target appear to bend away from normal on upper side of the interface. The equivalent target will be closer to the surface than the actual target, at a depth d''.

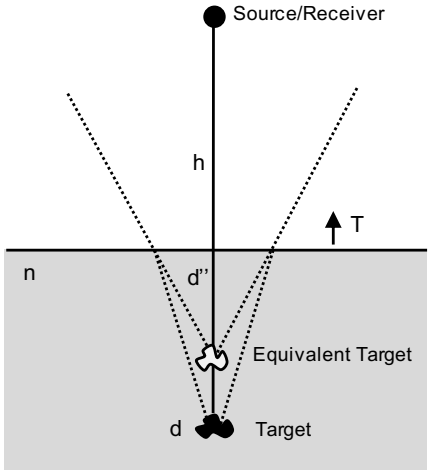

Fig. S14: Geometry for the equivalent subsurface target in free space.

Making a similar argument as before, the equivalent target must have the same power at the interface as radiated by the actual target. Treating the equivalent target as an equivalent source with transmit power, P_t'', the scattered power density from the equivalent target at the interface is

$$S'' = \frac{P_t''}{4\pi d''^2} \tag{S.84}$$

and the scattered power is

$$P'' = S'' A \tag{S.85}$$

Equating P'' and P_{++}, the equivalent target needs to radiate with power

$$P_t'' = P_\sigma T \frac{d''^2}{d^2} \tag{S.86}$$

The dielectric medium can now be replaced with free space and the equivalent target. The power density radiated from the equivalent target at the receiver is

$$S_r = \frac{P_t''}{4\pi (h + d'')^2} \tag{S.87}$$

The power received is

$$P_r = S_r A_r \tag{S.88}$$

Putting these all together

$$P_r = \frac{P_t''}{4\pi (h + d'')^2} \frac{G_r \lambda^2}{4\pi} \tag{S.89}$$

$$= P_\sigma T \frac{d''^2}{d^2} \frac{1}{4\pi (h + d'')^2} \frac{G_r \lambda^2}{4\pi} \tag{S.90}$$

$$= S_d \sigma_{\epsilon_r} T \frac{d''^2}{d^2} \frac{1}{4\pi (h + d'')^2} \frac{G_r \lambda^2}{4\pi} \tag{S.91}$$

$$= \frac{P_t G_t T}{4\pi (h' + d)^2} \frac{h'^2}{h^2} \sigma_{\epsilon_r} T \frac{d''^2}{d^2} \frac{1}{4\pi (h + d'')^2} \frac{G_r \lambda^2}{4\pi} \tag{S.92}$$

which becomes

$$P_r = \frac{P_t G_t G_r \lambda^2 T^2 \sigma_{\epsilon_r}}{(4\pi)^3 (h' + d)^2 (h + d'')^2} \frac{h'^2}{h^2} \frac{d''^2}{d^2} \tag{S.93}$$

The same Snell's law approximations are used as Section S2.1 for the equivalent source height and equivalent target depth:

$$h'/h = n \tag{S.94}$$

$$d''/d = 1/n \tag{S.95}$$

The equivalent source is higher than the original source by a factor of n, and the equivalent target is shallower than the actual target by a factor of $1/n$. Using these,

$$P_r = \frac{P_t G_t G_r \lambda^2 T^2 \sigma_{\epsilon_r}}{(4\pi)^3 (hn+d)^2 (h+d/n)^2} n^2 \frac{1}{n^2} \tag{S.96}$$

$$= \frac{P_t G_t G_r \lambda^2 T^2 \sigma_{\epsilon_r}}{(4\pi)^3 (h+d/n)^4} \frac{1}{n^2} \frac{(h+d)^4}{(h+d)^4} \tag{S.97}$$

After rearranging, the subsurface radar equation for spherical waves and arbitrary target under a flat interface is

$$P_r = \frac{P_t G_t G_r \lambda^2 T^2 \sigma_{\epsilon_r}}{(4\pi)^3 (h+d)^4} \frac{g_r^4}{n^2} \tag{S.98}$$

This has reduced to the standard radar equation modified by transmissivity, refraction gain, the index of refraction of the subsurface, and target radar cross section evaluated in the medium. Equation (S.98) has the same form as (Peters and others, 2005, Eq. 2). This radar equation is useful as a starting point to compute the power for arbitrary subsurface scattering objects at nadir. For example, rough basal interfaces at nadir for which the image equation does not apply and for which backscatter or normalized backscatter is a more appropriate characterization of the interface.

S2.4. Subsurface Off-Nadir - General Radar Equation - Spherical Waves - Flat Surface

This is the derivation for the radar equation for off-nadir subsurface targets for a flat surface interface, represented in Figure S15. The derivation follows the same steps as the power conservation and image methods in the previous section. This assumes that the location of the subsurface target is known and that a flat-surface refraction solution has been computed between the source and the target, such that the refraction point, incidence angle, θ_i, and transmission angle, θ_t, are known.

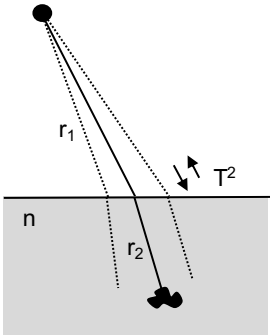

Fig. S15: Geometry for the equivalent subsurface target in free space.

The power density of the transmitting antenna at the refraction point on the surface is

$$S = \frac{P_t G_t}{4\pi r_1^2} \tag{S.99}$$

where r_1 is the distance between the source and refraction point. The total power incident over the projected area A on the surface is

$$P_+ = SA\cos\theta_i \tag{S.100}$$

The total power below the interface is

$$P_- = TP_+ \tag{S.101}$$

where T is the transmissivity evaluated at the incidence angle from the refraction solution. An equivalent source is placed at a height h', which is higher than the real source at height h above the surface. The geometry is shown in Figure S16. The distance from the equivalent source and the refraction point is r_1'. We want this source to radiate such that it has the same power as P_- at the refraction point. The power radiated by the equivalent source over the projected area in the subsurface is

$$P' = S'A\cos\theta_t = \frac{P_t' G' A \cos\theta_t}{4\pi r_1'^2} \tag{S.102}$$

where A is the illuminated area on the surface, S' is the power density of the equivalent source at the interface and $P_t'G'$ is the power-gain product of the equivalent source. Equating P_- and P' and solving for the power-gain product, $P_t'G'$, of the equivalent source

$$P_t'G' = P_t G_t T \frac{r_1'^2}{r_1^2} \frac{\cos\theta_i}{\cos\theta_t} \tag{S.103}$$

We can now replace the original source and free-space above the surface interface with the equivalent source in the medium. The waves are propagating with rays radiated from the equivalent source in the medium. The power density of equivalent source has the form

$$S' = \frac{P_t'G'}{4\pi R'^2} \tag{S.104}$$

The power density of the equivalent source at the target at a range of $r_1' + r_2$ is then

$$S' = \frac{P_t G_t T}{4\pi (r_1' + r_2)^2} \frac{r_1'^2}{r_1^2} \frac{\cos\theta_i}{\cos\theta_t} \tag{S.105}$$

where r_2 is the distance from the refraction point to the target. Note, the antenna gain and transmissivity are evaluated at the incident angle of the original source.

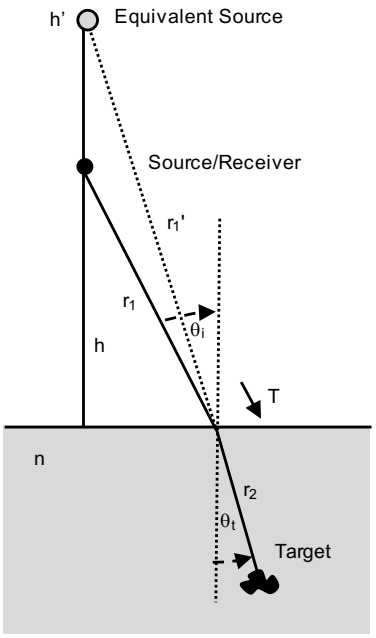

Fig. S16: Geometry for equivalent source/receiver in the medium of the subsurface.

The power scattered by the subsurface target is

$$P_\sigma = S'\sigma_{\epsilon_r} \tag{S.106}$$

where σ_{ϵ_r} is the radar backscatter of the target in a medium of ϵ_r. The scattered power density at the refraction point is then

$$S_\sigma = \frac{P_\sigma}{4\pi r_2^2} \tag{S.107}$$

The intercepted power at the surface over an area A is

$$P_{--} = S_\sigma A \cos\theta_t \tag{S.108}$$

and the power above the interface is

$$P_{++} = TP_{--} \tag{S.109}$$

As before, we replace the target with an equivalent target (or source) in order replace the dielectric subsurface with free-space, see Figure S17. It must be positioned so that the rays are in a straight line to the original source. The equivalent target is placed closer to the surface, along a vertical line between the target and the interface. The equivalent target must radiate the same power above the interface as radiated by the original target. The power radiated by the equivalent target over an area A at the interface is written as

$$P'' = S''A\cos\theta_i = \frac{P_t'' A\cos\theta_i}{4\pi r_2''^2} \tag{S.110}$$

where r_2'' is the distance between the equivalent target and the refraction point. Equating P_{++} and P'', the transmit power of the equivalent target is

$$P_t'' = P_\sigma T \frac{r_2''^2}{r_2^2}\frac{\cos\theta_t}{\cos\theta_i} \tag{S.111}$$

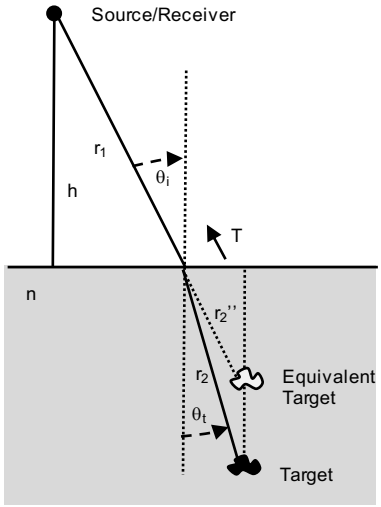

Fig. S17: Geometry for the equivalent subsurface target in free space.

The dielectric can now be replaced with vacuum and the equivalent target (source). The power density from the equivalent target at an arbitrary distance is

$$S_r = \frac{P_t''}{4\pi R''^2} \tag{S.112}$$

Using $R'' = r_1 + r_2''$, the power density at the receiver is

$$S_r = \frac{P_t''}{4\pi(r_1 + r_2'')^2} \tag{S.113}$$

The power received is

$$P_r = S_r A_r \tag{S.114}$$

Putting all these together, the received power is

$$P_r = \frac{P_t''}{4\pi(r_1 + r_2'')^2}\frac{G_r\lambda^2}{4\pi} \tag{S.115}$$

$$= P_\sigma T \frac{r_2''^2}{r_2^2}\frac{\cos\theta_t}{\cos\theta_i}\frac{1}{4\pi(r_1 + r_2'')^2}\frac{G_r\lambda^2}{4\pi} \tag{S.116}$$

$$= S'\sigma_{\epsilon_r} T \frac{r_2''^2}{r_2^2}\frac{\cos\theta_t}{\cos\theta_i}\frac{1}{4\pi(r_1 + r_2'')^2}\frac{G_r\lambda^2}{4\pi} \tag{S.117}$$

$$= \frac{P_t G_t T}{4\pi(r_1' + r_2)^2}\frac{r_1'^2}{r_1^2}\frac{\cos\theta_i}{\cos\theta_t}\sigma_{\epsilon_r} T \frac{r_2''^2}{r_2^2}\frac{\cos\theta_t}{\cos\theta_i}\frac{1}{4\pi(r_1 + r_2'')^2}\frac{G_r\lambda^2}{4\pi} \tag{S.118}$$

which becomes

$$P_r = \frac{P_t G_t G_r \lambda^2 T^2 \sigma_{\epsilon_r}}{(4\pi)^3(r_1' + r_2)^2(r_1 + r_2'')^2}\frac{r_1'^2}{r_1^2}\frac{r_2''^2}{r_2^2} \tag{S.119}$$

This is the same as (S.93) with the analogous terms interchanged: $[h, d, r', d''] = [r_1, r_2, r_1', r_2'']$. The cosine area projection terms cancel, as we expect from conservation of power.

The ranges of the equivalent source and target to the refraction point, r_1' and r_2'', are found by equating the common triangle edges along the surface formed by the

original source or target. The geometry is shown in Figure S18.

$$r_1' = r_1 \frac{\sin\theta_i}{\sin\theta_t} \tag{S.120}$$

$$r_2'' = r_2 \frac{\sin\theta_t}{\sin\theta_i} \tag{S.121}$$

Using these in (S.119)

$$P_r = \frac{P_t G_t G_r \lambda^2 T^2 \sigma_{\epsilon_r}}{(4\pi)^3 \left(r_1 \frac{\sin\theta_i}{\sin\theta_t} + r_2\right)^2 \left(r_1 + r_2 \frac{\sin\theta_t}{\sin\theta_i}\right)^2} \tag{S.122}$$

Multiplying top and bottom by $(r_1 + r_2)^4$ and rearranging

$$P_r = \frac{P_t G_t G_r \lambda^2 T^2 \sigma_{\epsilon_r}}{(4\pi)^3 (r_1 + r_2)^4} \frac{(r_1 + r_2)^4}{\left(r_1 + r_2 \frac{\sin\theta_t}{\sin\theta_i}\right)^4} \frac{\sin^2\theta_t}{\sin^2\theta_i} \tag{S.123}$$

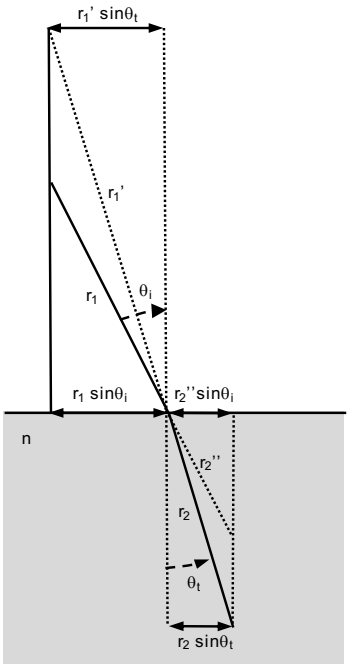

Fig. S18: Geometry for the ranges to the equivalent source and equivalent target.

After applying Snell's law, $\sin\theta_i = n \sin\theta_t$, this reduces to

$$P_r = \frac{P_t G_t G_r \lambda^2 T^2 \sigma_{\epsilon_r}}{(4\pi)^3 (r_1 + r_2)^4} \frac{g_r'^4}{n^2} \tag{S.124}$$

where g_r' is the refraction gain for off-nadir targets

$$g_r' = \frac{r_1 + r_2}{r_1 + r_2/n} \tag{S.125}$$

Equation (S.124) is the same radar equation as for the nadir subsurface targets, (S.98), with height and depth replaced by distances between source and target to the refraction point. Likewise, (S.125) is (S.75) with the same substitutions.

Like its normal-incident counterpart, this radar equation is useful to compute the received power from arbitrary subsurface scattering objects. In particular, this can be used for off-nadir, cross-track subsurface targets after along-track subsurface SAR focusing. These targets could be subsurface ridges, once they have been identified, or arbitrary targets used for radar system analysis when evaluating the effects of subsurface cross-track clutter.

S2.5. Subsurface - Fresnel Zone - Spherical Waves - Flat Surface - Flat Subsurface

Here we derive the radar equation for a subsurface Fresnel zone target with flat surface and subsurface interfaces for spherical wave incidence. The geometry is represented in Figure S19. The equation is derived by integrating the surface phase integral over the subsurface Fresnel zone.

The radar cross section for a subsurface disk at normal incidence with spherical wave fronts under the Kirchhoff approximation is

$$\sigma_{disk} = \Gamma \frac{4\pi |I|^2}{\lambda_{\epsilon_r}^2} \tag{S.126}$$

where λ_{ϵ_r} is the wavelength in the medium and the reflectivity, Γ, is understood to apply to the subsurface interface.

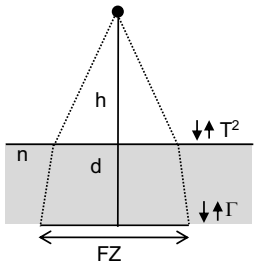

Fig. S19: Geometry for the subsurface Fresnel zone with spherical waves and flat surface and flat subsurface.

The geometry is shown in Figure S20. The phase integral over the subsurface target is

$$I = \int_0^{2\pi} \int_0^a e^{i2k(l_1 + n l_2)} \rho d\rho d\theta \tag{S.127}$$

where ρ and θ are the integration variables over the subsurface disk, l_1 is the ray distance from the source to a refraction point on the surface interface, l_2 is the ray distance from the refraction point to a subsurface interface, and k is the free-space wavenumber. This expression integrates the two-way electrical length $l_1 + n l_2$ over the subsurface target. The first maximum of this phase integral is the first subsurface Fresnel zone.

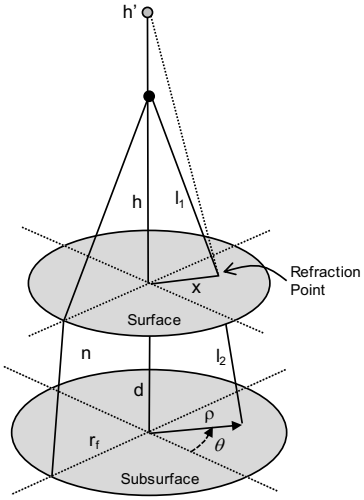

Fig. S20: Geometry for the subsurface Fresnel zone phase integral for spherical waves and flat surface and flat subsurface.

The distances l_1 and l_2 are functions of the integration variable ρ and satisfy Snell's law at the interface. For a sensor at height, h, and interface at depth, d, then from the geometry

$$l_1^2 = h^2 + x^2 \tag{S.128}$$
$$l_2^2 = d^2 + (\rho - x)^2 \tag{S.129}$$

where x is the refraction point in the horizontal plane, yet to be determined. The solution of x using Snell's law is nonlinear. To proceed, we use the same approximation as before, where the source is replaced with an equivalent source at height $h' = hn$, such that the subsurface rays appear to radiate from this source. From similar triangles, Figure S20,

$$\frac{x}{\rho} = \frac{h'}{h' + d} \tag{S.130}$$

Solving for the refraction point

$$x = \rho \frac{h}{h + d/n} \tag{S.131}$$

then the ray distances are

$$l_1^2 = h^2 + \rho^2 b^2 \tag{S.132}$$
$$l_2^2 = d^2 + \rho^2 (1-b)^2 \tag{S.133}$$
$$b = \frac{h}{h + d/n} \tag{S.134}$$

or

$$l_1 = \sqrt{h^2 + \rho^2 b^2} \tag{S.135}$$
$$l_2 = \sqrt{d^2 + \rho^2 (1-b)^2} \tag{S.136}$$

The square roots must be approximated to complete the integral. Assuming that $h \gg \rho b$, and $d \gg \rho(1-b)$, the square roots are expanded with $c\sqrt{1 + x^2/c^2} \approx c + x^2/2c$

$$l_1 \approx h + \frac{\rho^2 b^2}{2h} \tag{S.137}$$
$$l_2 \approx d + \frac{\rho^2 (1-b)^2}{2d} \tag{S.138}$$

Substituting these into (S.127) and evaluating the θ integral

$$I \approx 2\pi \int_0^a e^{i2k(h + \rho^2 b^2/2h + n(d + \rho^2(1-b)^2/2d))} \rho d\rho \tag{S.139}$$
$$= 2\pi \int_0^a e^{i2k(A + B\rho^2)} \rho d\rho \tag{S.140}$$

where the constants reduce to

$$A = h + nd \tag{S.141}$$
$$B = \frac{b^2}{2h} + \frac{n(1-b)^2}{2d} \tag{S.142}$$
$$= \frac{1}{2(h + d/n)} \tag{S.143}$$

The integral (S.140) is evaluated as

$$I = -\frac{2\pi i}{4kB} e^{i2kA} \left(-1 + e^{i2ka^2 B} \right) \tag{S.144}$$

The magnitude is

$$|I| = \frac{2\pi}{4kB} \left| -1 + e^{i2ka^2 B} \right| \tag{S.145}$$

and the magnitude squared is

$$|I|^2 = \frac{4\pi^2}{(4kB)^2} \left| -1 + e^{i2ka^2 B} \right|^2 \tag{S.146}$$
$$= \frac{4\pi^2}{(4kB)^2} \left(2 - 2\cos\left(2ka^2 B \right) \right) \tag{S.147}$$
$$= \frac{2\pi^2 (h + d/n)^2}{k^2} \left(1 - \cos\left(\frac{ka^2}{h + d/n} \right) \right) \tag{S.148}$$

Equation (S.146) is maximized when

$$2ka^2 B = \pi m, \quad m \text{ odd} \tag{S.149}$$

Evaluated at $m = 1$,

$$a^2 = \pi/(2kB) \tag{S.150}$$
$$= \frac{\pi}{2k} 2(h + d/n) \tag{S.151}$$
$$= \frac{\lambda}{2}(h + d/n) \tag{S.152}$$

Therefore, the radius of the subsurface Fresnel zone for flat surface interface and flat subsurface interface is, approximately, (Peters and others, 2005),

$$r_f \approx \sqrt{\frac{\lambda}{2}\left(h + \frac{d}{n} \right)} \tag{S.153}$$

This is analogous to the surface Fresnel zone with $h \to h + d/n$. Evaluating (S.148) at the subsurface Fresnel zone radius, the magnitude squared of the phase integral is

$$|I|^2 = \frac{4\pi^2 (h + d/n)^2}{k^2} \tag{S.154}$$

Using this in (S.126), the radar backscatter for the Fresnel zone for a flat subsurface interface at depth d is

$$\sigma_{\epsilon_r}(a = r_f) = \Gamma \frac{4\pi |I|^2}{\lambda_{\epsilon_r}^2} \tag{S.155}$$
$$= \Gamma \frac{4\pi n^2}{\lambda^2} \frac{4\pi^2 (h + d/n)^2}{k^2} \tag{S.156}$$
$$= \Gamma 4\pi n^2 (h + d/n)^2 \tag{S.157}$$

Using (S.157) in the radar equation for arbitrary subsurface targets at nadir, (S.98), the received power from the subsurface Fresnel zone is

$$P_r = \frac{P_t G_t G_r \lambda^2 T^2 \Gamma 4\pi n^2 (h + d/n)^2}{(4\pi)^3 (h+d)^4} \frac{g_r^4}{n^2} \tag{S.158}$$

Simplifying, the radar equation for the subsurface Fresnel zone and spherical waves is

$$P_r = \frac{P_t G_t G_r \lambda^2 T^2 \Gamma}{(4\pi)^2 (h+d)^2} g_r^2 \tag{S.159}$$

The constant in the denominator is the same as the analogous expression for the surface Fresnel zone, with the addition of the refraction gain and transmissivity.

For flat interfaces, this radar equation is recommended for subsurface link budgets of Fresnel zone sized targets because it includes spherical waves and refraction gain. Note, the received power will be less than (S.159) if the target size is larger or smaller than the Fresnel zone. Like its surface counterpart, (S.28), this equation can be used if one wants to compute the received power of a Fresnel zone sized target after, for instance, along-track SAR focusing.

S2.6. Subsurface Fresnel Zone - Plane Waves or 'Antenna' Approach - Flat Surface - Flat Subsurface

This derivation is for a subsurface Fresnel zone using the plane wave or 'antenna' approach. This is represented in Figure S21. The backscatter for a disk in a medium of ϵ_r with normal plane wave incidence is

$$\sigma_{disk} = \Gamma \frac{4\pi A^2}{\lambda_{\epsilon_r}^2} \tag{S.160}$$

where the surface phase integral reduces to the disk area.

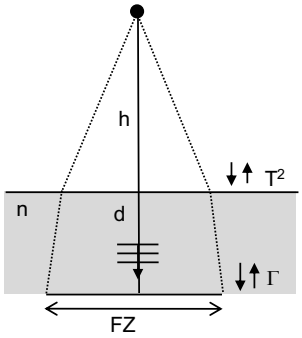

Fig. S21: Geometry for the subsurface Fresnel zone and plane wave incidence.

Using (S.153) for the Fresnel zone radius in the subsurface through a flat surface interface, the backscatter from the Fresnel zone in the medium is

$$\sigma_{\epsilon_r} = \Gamma \frac{4\pi \pi^2 r_f^4}{\lambda_{\epsilon_r}^2} \tag{S.161}$$

$$= \Gamma \frac{4\pi}{\lambda_{\epsilon_r}^2} \pi^2 \frac{\lambda^2}{4} \left(h + \frac{d}{n}\right)^2 \tag{S.162}$$

$$= \Gamma \pi^3 n^2 (h + d/n)^2 \tag{S.163}$$

Substituting this into (S.98)

$$P_r = \frac{P_t G_t G_r \lambda^2 T^2 \Gamma \pi^3 n^2 (h + d/n)^2}{(4\pi)^3 (h+d)^4} \frac{(h+d)^4}{(h+d/n)^4 n^2} \tag{S.164}$$

$$= \frac{P_t G_t G_r \lambda^2 T^2 \Gamma}{4^3 (h+d)^2} \frac{(h+d)^2}{(h+d/n)^2} \tag{S.165}$$

Simplifying, the received power from a subsurface Fresnel zone using the plane wave incidence is

$$P_r = \frac{P_t G_t G_r \lambda^2 T^2 \Gamma}{4^3 (h+d)^2} g_r^2 \tag{S.166}$$

This has the same denominator constant as the analogous plane-wave case for Fresnel zone surface targets, Section S1.6. It also has the same refractive gain as the image method, because the same small angle approximation is used for the height of the image sources as the one used to derive the Fresnel zone radius.

S2.7. Subsurface Fresnel Zone - Spherical Waves - Spherical Surface - Spherical Subsurface

This is a derivation of the Fresnel zone and radar equation for a spherical subsurface interface. This exercise is to understand what approximations need to be made to arrive at analytic expressions for this geometry.

The geometry is shown in Figure S22. The surface phase integral of a spherical subsurface target at depth, d, through a spherical surface with radius, r, is written in spherical coordinates as

$$I = \int_0^{2\pi} \int_0^{\beta} e^{i2k(l_1 + n l_2)} (r-d)^2 \sin\theta d\theta d\phi \tag{S.167}$$

where l_1 is the ray path lengths from the source to the refraction point on the surface, and l_2 is the ray path from the refraction point to the integration point on the subsurface. This has the same form as (S.127) but evaluated over the sphere of the subsurface. The radius of the subsurface sphere is $r-d$ and β is the limit of the θ integration on the subsurface sphere. Let α be the angle between the z-axis and the vector from the center of the sphere to the refraction point at the surface interface. From the law of cosines

$$l_1^2 = r^2 + (r+h)^2 - 2r(r+h)\cos\alpha \tag{S.168}$$

$$l_2^2 = r^2 + (r-d)^2 - 2r(r-d)\cos(\theta - \alpha) \tag{S.169}$$

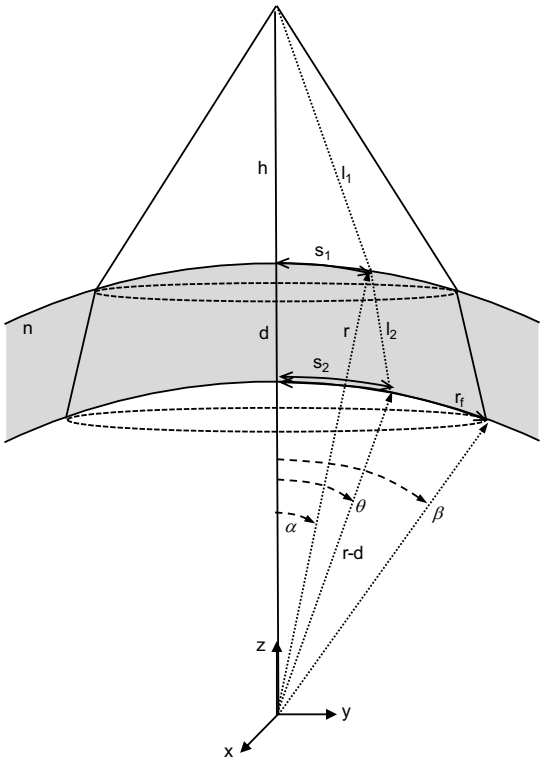

Fig. S22: Geometry for the subsurface Fresnel zone with spherical surface and spherical subsurface.

Let the arc lengths from the surface nadir point to the transmission point, and from the subsurface nadir point to the integration point be s_1 and s_2, respectively. Analogous to the approximation made for refraction through a flat surface with flat subsurface, we let the ratio of these two arc lengths be equal to the same ratio as when the interfaces are parallel. This applies when the radius of the sphere is large compared to the sensor height and subsurface interface depth. The ratio of the arc lengths is

$$\frac{s_1}{s_2} = \frac{r\alpha}{(r-d)\theta} \tag{S.170}$$

The arc lengths are approximated using the geometry in Section S2.5 for an equivalent source over a flat interface, (S.130), as

$$\frac{s_1}{s_2} \approx \frac{h'}{h'+d} = \frac{hn}{hn+d} = \frac{h}{h+d/n} \tag{S.171}$$

where $h' = hn$ is the height of the equivalent source over a flat interface. Equating (S.170) and (S.171) we solve for α in terms of the integration angle

$$\alpha \approx \theta \frac{r-d}{r}\frac{h}{h+d/n} \tag{S.172}$$

Substituting this into l_1 and l_2

$$l_1 = \sqrt{r^2 + (r+h)^2 - 2r(r+h)\cos\left(\theta\frac{r-d}{r}\frac{h}{h+d/n}\right)} \tag{S.173}$$

$$l_2 = \sqrt{r^2 + (r-d)^2 - 2r(r-d)\cos\left(\theta\frac{d(hn+r)}{r(hn+d)}\right)} \tag{S.174}$$

Assuming θ is small, expanding first the cosine and then the square root gives

$$l_1 \approx h + \theta^2\frac{hn^2(d-r)^2(r+h)}{2r(d+hn)^2} \tag{S.175}$$

$$l_2 \approx d + \theta^2\frac{d(r-d)(hn+r)^2}{2r(d+hn)^2} \tag{S.176}$$

Using these in the electrical path $l_1 + nl_2$ and collecting terms

$$l_1 + nl_2 = A + B\theta^2 \tag{S.177}$$

where

$$A = h + nd \tag{S.178}$$

$$B = \frac{hn^2(d-r)^2(r+h) + nd(r-d)(hn+r)^2}{2r(d+hn)^2} \tag{S.179}$$

Substituting (S.177) into (S.167), approximating $\sin\theta \approx \theta$, and evaluating the ϕ integral, the phase integral becomes

$$I \approx 2\pi\int_0^\beta e^{i2k(A+B\theta^2)}(r-d)^2\theta d\theta \tag{S.180}$$

which is evaluated as

$$I = -2\pi(r-d)^2\frac{1}{4kB}ie^{2iAk}(-1+e^{2i\beta^2Bk}) \tag{S.181}$$

The magnitude of the phase integral is

$$|I| = 2\pi(r-d)^2\frac{1}{4kB}\left|-1+e^{2i\beta^2Bk}\right| \tag{S.182}$$

This is maximized when

$$2\beta^2Bk = m\pi \tag{S.183}$$

Therefore, the integration limit that corresponds to the first Fresnel zone on the subsurface interface is

$$\beta^2 = \frac{\pi}{2kB} \tag{S.184}$$

$$= \frac{\pi}{2k}\frac{2r(d+hn)^2}{hn^2(d-r)^2(r+h) + nd(r-d)(hn+r)^2} \tag{S.185}$$

$$= \frac{\lambda}{2}(h+d/n)\frac{rn^2(h+d/n)}{hn^2(d-r)^2(r+h) + nd(r-d)(hn+r)^2} \tag{S.186}$$

The Fresnel radius on the subsurface interface is the arc length $s = (r-d)\beta$, or

$$r_f = \sqrt{\frac{\lambda}{2}(h+d/n)\frac{nr(r-d)(h+d/n)}{hn(r-d)(r+h) + d(hn+r)^2}} \tag{S.187}$$

This is the same as the Fresnel zone radius for the flat subsurface interface, (S.153), except with a correction factor

for refraction through the spherical surface interface and Fresnel zone of the spherical subsurface. Note, several versions of this derivation were attempted and (S.187) best matched the numerical solution for this Fresnel zone.

Checking the limits of (S.187). When $r \to \infty$,

$$r_f = \sqrt{\frac{\lambda}{2}(h+d/n)\frac{r(r-d)^2n^2(h+d/n)}{hn^2(d-r)^2(r+h)+nd(r-d)(hn+r)^2}} \tag{S.188}$$

$$= \sqrt{\frac{\lambda}{2}(h+d/n)\frac{r^3n^2(h+d/n)}{hn^2r^3+ndr^3}} \tag{S.189}$$

$$= \sqrt{\frac{\lambda}{2}(h+d/n)\frac{n^2(h+d/n)}{hn^2+nd}} \tag{S.190}$$

$$= \sqrt{\frac{\lambda}{2}(h+d/n)} \tag{S.191}$$

which is (S.153) for a flat interface. When $d \to 0$,

$$r_f = \sqrt{\frac{\lambda}{2}(h+d/n)\frac{r(r-d)^2n^2(h+d/n)}{hn^2(d-r)^2(r+h)+nd(r-d)(hn+r)^2}} \tag{S.192}$$

$$= \sqrt{\frac{\lambda}{2}h\frac{r^3n^2h}{hn^2r^2(r+h)}} \tag{S.193}$$

$$= \sqrt{\frac{\lambda}{2}\frac{rh}{(r+h)}} \tag{S.194}$$

which is (S.46) for a spherical surface. When $n \to 1$

$$r_f = \sqrt{\frac{\lambda}{2}(h+d/n)\frac{r(r-d)^2n^2(h+d/n)}{hn^2(d-r)^2(r+h)+nd(r-d)(hn+r)^2}} \tag{S.195}$$

$$= \sqrt{\frac{\lambda}{2}(h+d)\frac{r(r-d)^2(h+d)}{h(d-r)^2(r+h)+d(r-d)(h+r)^2}} \tag{S.196}$$

$$= \sqrt{\frac{\lambda}{2}(h+d)\frac{r(r-d)^2(h+d)}{(h+r)r(d+h)(-d+r)}} \tag{S.197}$$

$$= \sqrt{\frac{\lambda}{2}\frac{(r-d)(h+d)}{(h+r)}} \tag{S.198}$$

$$= \sqrt{\frac{\lambda}{2}\frac{(r-d)(d+h)}{(h+d+r-d)}} \tag{S.199}$$

$$= \sqrt{\frac{\lambda}{2}\frac{r'h'}{r'+h'}} \tag{S.200}$$

which is (S.46) for a spherical interface and no medium, where the sensor altitude is $h' = h + d$ and the body radius is $r' = r - d$.

The magnitude of the surface phase integral evaluated at the Fresnel zone radius is

$$|I| = \pi(r-d)^2\frac{1}{kB} \tag{S.201}$$

$$= \frac{\pi}{k}\frac{2r(r-d)n(h+d/n)^2}{hn(r-d)(r+h)+d(hn+r)^2} \tag{S.202}$$

The magnitude squared of the surface phase integral is

$$|I|^2 = \frac{\pi^2}{k^2}\left(\frac{2r(r-d)n(h+d/n)^2}{hn(r-d)(r+h)+d(hn+r)^2}\right)^2 \tag{S.203}$$

Substituting (S.203) into the backscatter of the subsurface target, (S.126),

$$\sigma_{\epsilon_r} = \Gamma\frac{4\pi|I|^2}{\lambda_{\epsilon_r}^2} \tag{S.204}$$

$$= \Gamma\frac{4\pi n^2}{\lambda^2}\frac{\pi^2}{k^2}\left(\frac{2r(r-d)n(h+d/n)^2}{hn(r-d)(r+h)+d(hn+r)^2}\right)^2 \tag{S.205}$$

$$= \Gamma 4\pi n^2(h+d/n)^2\left(\frac{r(r-d)n(h+d/n)}{hn(r-d)(r+h)+d(hn+r)^2}\right)^2 \tag{S.206}$$

Then using (S.206) in (S.98) for the arbitrary subsurface target, the received power is

$$P_r = \frac{P_tG_tG_r\lambda^2T^2}{(4\pi)^3(h+d)^4}\frac{g_r^4}{n^2}\Gamma 4\pi n^2(h+d/n)^2 \cdot\left(\frac{r(r-d)n(h+d/n)}{hn(r-d)(r+h)+d(hn+r)^2}\right)^2 \tag{S.207}$$

$$= \frac{P_tG_tG_r\lambda^2T^2\Gamma}{(4\pi)^2(h+d)^2}g_r^2\frac{(r-d)^2}{((r-d)+(h+d))^2} \cdot\left(\frac{r(r+h)n(h+d/n)}{hn(r-d)(r+h)+d(hn+r)^2}\right)^2 \tag{S.208}$$

The last step extracts the correction term for the spherical subsurface.

Summary The radar equation for spherical incident waves, spherical surface, spherical subsurface Fresnel zone, including refraction through the spherical surface, is:

$$P_r = \underbrace{\frac{P_tG_tG_r\lambda^2T^2\Gamma}{(4\pi)^2(h+d)^2}}_{1}\underbrace{g_r^2}_{2}\underbrace{\frac{(r-d)^2}{((r-d)+(h+d))^2}}_{3} \cdot\underbrace{\left(\frac{r(r+h)n(h+d/n)}{hn(r-d)(r+h)+d(hn+r)^2}\right)^2}_{4} \tag{S.209}$$

This is composed of four parts and represented in Figure S23:

1. Radar equation for a flat Fresnel zone target at $h + d$, (S.28), with the addition of transmissivity.
2. Refraction gain through a flat surface, (S.75). This term matters more when the altitude is low and the target is deep.
3. Spherical surface correction (i.e., $r^2/(r+h)^2$, (S.57)) applied to a spherical subsurface with radius $(r - d)$ and sensor altitude $(h + d)$. Of the terms 2, 3, and 4, this term contributes the most loss, especially at high sensor altitudes or large depths relative to the body radius.
4. Correction factor for the subsurface Fresnel zone that includes the effects of spherical waves, refraction through spherical surface, and Fresnel zone radius of the subsurface spherical target. This term contributes between [0, -0.1] dB across a wide range of parameters and in most cases can be ignored. More specifically, this term contributes little if $d \ll r$ (regardless of the value of h and r) and is only significant when neither $d \ll r$ nor $h \ll d$ are valid, for which the only related practical applications

would be radar sounders orbiting comparatively small objects, such as icy comets or asteroids, albeit spherical in shape with spherical subsurface interfaces.

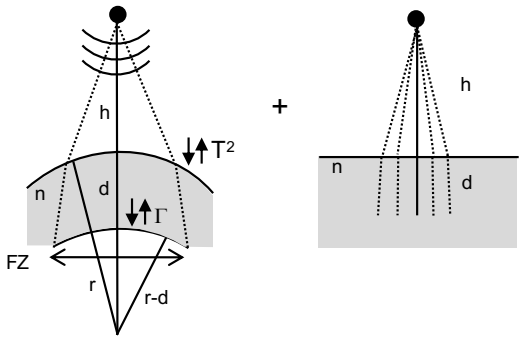

Fig. S23: Representation of the factors in Equation (S.209): refraction-correction for the subsurface Fresnel zone and flat surface refraction gain.

Ignoring the spherical subsurface correction factor, term #4 in (S.209), the simplest radar equation which is recommended for a Fresnel zone subsurface target with spherical incident waves and spherical interfaces is

$$P_r = \frac{P_t G_t G_r \lambda^2 T^2 \Gamma}{(4\pi)^2 (h+d)^2} g_r^2 \frac{(r-d)^2}{((r-d)+(h+d))^2} \quad \text{(S.210)}$$

This emphasizes the fact that the spherical surface correction is applied to a sphere with radius $r-d$ and sensor altitude $h+d$. Refraction is only captured by g_r, which is for a flat surface, and is not applied to the subsurface Fresnel zone radius. This is represented in Figure S24.

A practical application in which to use (S.210) is in the case of spherically idealized ice-ocean interfaces that are sounded from orbit on Europa or Ganymede, where the interfaces are assumed specular and equal in size to the Fresnel zone.

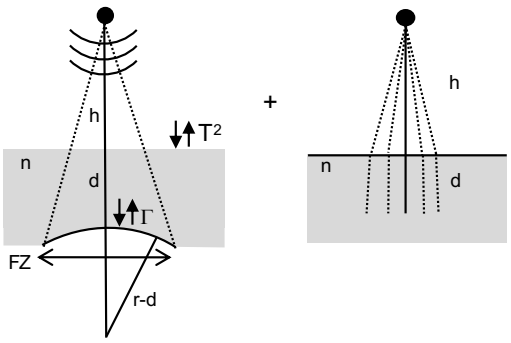

Fig. S24: Representation of the factors in Equation (S.210): uncorrected subsurface Fresnel zone and flat-surface refraction gain.

S3. PULSE LIMITED

Here we derive the radar equations for pulse limited targets and nadir incidence. The Fresnel zone is usually taken as the limiting size for specular (flat and smooth) surfaces at nadir, while the pulse limited area is used for rough surfaces or off-nadir targets. The geometric fall-off of incoherent, pulse limited targets goes as $1/R^3$, rather than the $1/R^2$ fall-off for purely specular, Fresnel zone sized targets, (Haynes and others, 2018), examples of which are real-aperture radar (Ulaby and others, 2014) and ocean altimetry (Brown, 1977; Hayne, 1980). The reason for this is that the backscatter of specular targets is proportional to area squared, while the backscatter of incoherent targets is only proportional to area.

These equations should be used for any surface or subsurface interface where 1) the roughness is comparable to the wavelength of the radar, 2) the backscatter can be reasonably estimated or assumed, or 3) the topographic variation within the antenna footprint at nadir is larger than the range resolution, but the backscatter can still be estimated within the range resolution cell. Depending on the radar parameters, examples of these cases can include crevassed ice, rough basal interfaces, and planetary surfaces (e.g., Mars polar ice caps, Europa).

S3.1. Pulse Limited - Spherical Waves - Flat Surface

For pulse-limited surface targets at normal incidence, one can replace $\lambda/2 \rightarrow 2\Delta\rho$ in the Fresnel zone radius to arrive at the pulse-limited radius, where $\Delta\rho$ is the range resolution of the radar. See Figure S25. This is demonstrated by comparing the pulse limited radius to the Fresnel zone radius as:

$$r_p = \sqrt{(h+\Delta\rho)^2 - h^2} \quad \text{(S.211)}$$

$$\approx \sqrt{2\Delta\rho h} \quad \text{(S.212)}$$

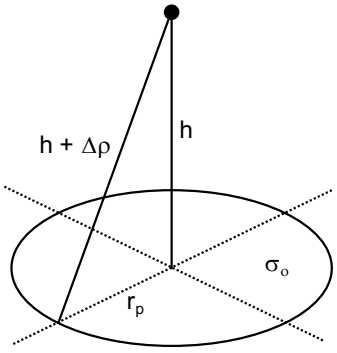

Fig. S25: Geometry for the pulse limited target.

Note, the pulse limited radius is always larger than the Fresnel zone (assuming that the maximum bandwidth of the radar is no greater than twice the center frequency). Using this to compute the area of a disk in the radar equation for incoherent targets, (S.2), gives

$$P_r = \frac{P_t G_t G_r \lambda^2 \sigma_o \Delta\rho}{2^5 \pi^2 h^3} \quad \text{(S.213)}$$

Equation (S.213) shows the well known $1/R^3$ geometric fall-off for incoherent targets. A similar form can be found in

(Haynes and others, 2018; Moore and Williams, 1957) as well as (Ulaby and others, 2014, Eq. 14.6) for side-looking real aperture radar. This equation assumes that the normalized backscatter, σ_o, which is in general a function of incident angle, is constant over the disk or, equivalently, that the average backscatter is used. More complete expressions that integrate the backscatter and antenna gain as a function of incident angle are found throughout the literature, some examples are (Ulaby and others, 2014; Fung and Eom, 1983; Moore and Williams, 1957; Hayne, 1980).

S3.2. Pulse Limited - Spherical Waves - Spherical Surface

The pulse limited radius over a spherical surface for normal incidence is found substituting $\lambda/2 \rightarrow 2\Delta\rho$ into (S.46),

$$r_p \approx \sqrt{\frac{2\Delta\rho h r}{(h+r)}} \tag{S.214}$$

See Figure S26. Using this to compute the area of a target with circular area in (S.2) we get

$$P_r = \frac{P_t G_t G_r \lambda^2 \sigma_o \Delta\rho}{2^5 \pi^2 h^3} \frac{r}{h+r} \tag{S.215}$$

which is similar to (S.213) with a correction for the spherical surface and incoherent targets. Just as the geometric fall-off goes a $1/R^3$ for incoherent targets, there is only one factor of the spherical correction, $r/(h+r)$, in contrast to (S.56) for fully coherent Fresnel zone which is multiplied by the square of the correction term. This radar equation is applicable to surface scattering in planetary radar sounding where the altitude of operation is comparable to the body radius.

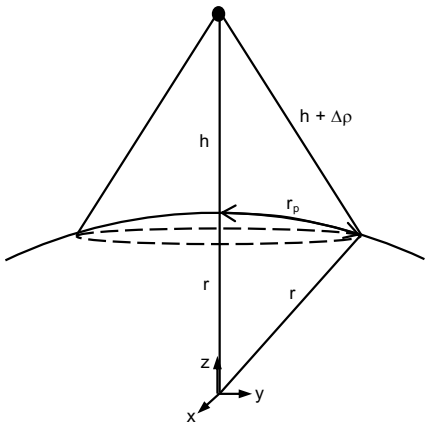

Fig. S26: Geometry for the pulse limited target.

S3.3. Pulse Limited - Spherical Waves - Flat Surface - Flat Subsurface

The pulse limited area for a flat subsurface is found by substituting $\lambda/2 \rightarrow 2\Delta\rho$ into the Fresnel zone for a flat subsurface, (S.153),

$$r_p = \sqrt{2\Delta\rho \left(h + \frac{d}{n}\right)} \tag{S.216}$$

See Figure S27. Using $\sigma_{\epsilon_r} = \sigma_{o,\epsilon_r} A$, where σ_{o,ϵ_r} is the normalized radar backscatter in the subsurface medium, and A is the area of disk, the backscatter of the pulse limited area in the medium is

$$\sigma_{\epsilon_r} = \sigma_{o,\epsilon_r} \pi 2\Delta\rho \left(h + \frac{d}{n}\right) \tag{S.217}$$

Substituting this into the general subsurface radar equation, (S.98),

$$P_r = \frac{P_t G_t G_r \lambda^2 T^2 \sigma_{o,\epsilon_r} A}{(4\pi)^3 (h+d)^4} \frac{g_r^4}{n^2} \tag{S.218}$$

$$= \frac{P_t G_t G_r \lambda^2 T^2 \sigma_{o,\epsilon_r}}{2^5 \pi^2 (h+d)^4} \Delta\rho \left(h + \frac{d}{n}\right) \frac{g_r^4}{n^2} \tag{S.219}$$

Therefore, the radar equation for a pulse limited subsurface incoherent target is

$$P_r = \frac{P_t G_t G_r \lambda^2 T^2}{2^5 \pi^2 (h+d)^3} g_r^3 \frac{\sigma_{o,\epsilon_r} \Delta\rho}{n^2} \tag{S.220}$$

This falls off as $(h+d)^3$ and is proportional to the refraction gain cubed. This radar equation is applicable to rough subsurface interfaces, especially in airborne radar sounder if the ice and basal interfaces are assumed to be flat and parallel.

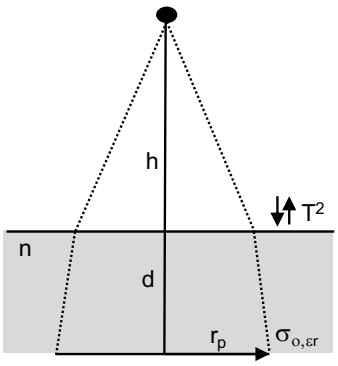

Fig. S27: Geometry for a subsurface pulse limited target.

S3.4. Pulse Limited - Spherical Waves - Flat Surface - Spherical Subsurface

Similar to (S.210), we can approximate the effects of the spherical subsurface by simply evaluating the spherical surface correction at the subsurface. Multiplying (S.220) by the spherical surface correction in (S.215) evaluated at $r \rightarrow r-d$ and $h \rightarrow h+d$, the radar equation for pulse-limited spherical subsurface is

$$P_r = \frac{P_t G_t G_r \lambda^2 T^2}{2^5 \pi^2 (h+d)^3} g_r^3 \frac{\sigma_{o,\epsilon_r} \Delta\rho}{n^2} \frac{(r-d)}{(h+d)+(r-d)} \tag{S.221}$$

which uses the refraction gain through a flat interface. This is represented in Figure S28. Note, refraction is not used to correct the pulse limited area.

This radar equation is applicable when the sensor altitude is comparable to the body radius and a spherical subsurface is assumed and the correction factor needed. Examples include spherically idealized ice-ocean interfaces that are sounded from orbit on Europa or Ganymede assuming the interfaces are rough.

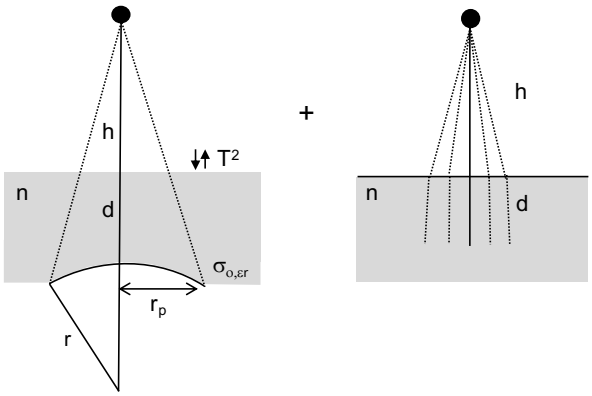

Fig. S28: Representation of the factors in Equation (S.221): spherical subsurface correction and flat surface refraction gain.

S4. PASSIVE SOUNDING

In passive radar sounding, natural or astronomical sources of low frequency radio noise (e.g., HF or VHF) are used in place of a transmitted incident field (Cecconi and others, 2012; Romero-Wolf and others, 2015; Schroeder and others, 2016; Peters and others, 2018). The radar simultaneously records the direct signal as it passes the radar and the same signal reflected from the target shifted in time. Range compression is accomplished by autocorrelating the digitized waveform which reveals a peak for both the direct and the reflected signals. Radar equations for this geometry are changed significantly by the fact that the wavefront of the radio noise is planar and constant when it incidents both the radar and the target. The following derivations give radar equations and Fresnel zones for passive sounding geometries.

S4.1. Passive Radar Equations

In passive sounding, the same plane wave that passes the instrument is incident on the target. The radar equations for the direct and reflected signals are

$$P_d = \frac{SG_d\lambda^2}{4\pi} \tag{S.222}$$

$$P_r = \frac{SG_r\lambda^2\sigma}{(4\pi)^2R^2} \tag{S.223}$$

where S is the power density of the plane wave, G_d and G_r are the gain of the antenna towards the source and the target, respectively. This is represented in Figure S29.

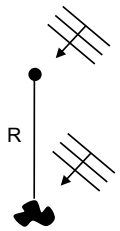

Fig. S29: Geometry for the general passive sounding radar equations.

Derivation

Let the power density of the incident field as it passes the receiver be S. The received power of the direct signal is then

$$P_d = SA_d \tag{S.224}$$

where A_d is the effective aperture of antenna while receiving the direct signal. The power density incident on the target is also S. The power intercepted by the target is

$$P_i = S\sigma \tag{S.225}$$

This is reradiated with power density

$$S_r = \frac{P_i}{4\pi R^2} \tag{S.226}$$

The power intercepted by the receive antenna is as before

$$P_r = S_rA_r \tag{S.227}$$

where A_r is the effective aperture of the antenna in the direction of the target. Putting these together, the power received from the target is then

$$P_r = \frac{SG_r\lambda^2\sigma}{(4\pi)^2R^2} \tag{S.228}$$

This shows that the power fall-off in passive sounding goes as R^2 rather than R^4.

S4.2. Passive - Fresnel Zone - Normal Plane Wave Incidence - Spherical Scattering - Flat Surface

In passive sounding, the incident field is a plane wave, but the waves scattered from the target are spherical. For Fresnel zone scattering, the surface phase integral is computed using the one-way phase over a disk. See Figure S30. The one-way phase integral for a normal incidence plane wave over a flat surface disk is

$$I = \int_0^{2\pi}\int_0^a e^{ik\sqrt{h^2+\rho^2}}\rho d\rho d\theta \tag{S.229}$$

where h is the height of the receiver above the surface. The integration will be identical to the Fresnel zone derivation for the active case over a flat surface with $k \to k/2$, or $\lambda \to 2\lambda$. Therefore, the Fresnel zone radius for normal incident passive sounding when $h \gg \lambda$ is

$$r_f = \sqrt{\lambda h} \tag{S.230}$$

$$= \sqrt{\frac{\lambda}{2}(2h)} \tag{S.231}$$

which is the same result as the Fresnel zone for the active case with $h \rightarrow 2h$. In other words, the passive sounder receiver appears to be at twice the height compared to the active sounding source when determining the Fresnel zone radius. Alternatively, the Fresnel zone boundary is a distance of $h + \lambda/2$ from the receiver. Equation (S.230) appears in (Schroeder and others, 2016).

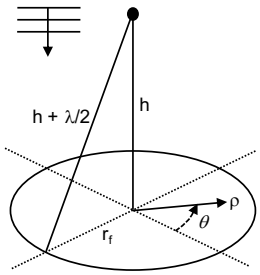

Fig. S30: Geometry for the general passive sounding radar equations.

The magnitude squared of the surface phase integral evaluated at the passive sounding Fresnel zone radius is, using (S.26),

$$|I|^2 = \frac{16\pi^2}{k^2}h^2 \tag{S.232}$$

The backscatter for the disk is again, (S.10),

$$\sigma_{disk} = \Gamma\frac{4\pi|I|^2}{\lambda^2} \tag{S.233}$$

Using (S.232) gives

$$\sigma_{disk}(a = r_f) = 16\pi\Gamma h^2 \tag{S.234}$$

Then using (S.234) in (S.223), with $R = h$, the radar equation for the reflected passive signal over the Fresnel zone for normal incidence and flat surface is

$$P_r = \frac{SG_r\lambda^2\Gamma}{\pi} \tag{S.235}$$

This does not depend on altitude and has therefore reduced to the equivalent of a 1D scattering problem, so long as the target being considered is always Fresnel zone sized.

S4.3. Passive - Fresnel Zone - Normal Plane Wave Incidence - Plane Wave Scattering - Flat Surface

Using the normal incident passive sounding Fresnel zone, (S.231), in the equation for the backscatter for plane wave incidence, (S.11), the backscatter assuming plane wave scattering at the target (i.e., without considering the surface phase integral to the receiver) is

$$\sigma_{disk} = \Gamma\frac{4\pi A^2}{\lambda^2} \tag{S.236}$$

$$= \Gamma\frac{4\pi(\pi\lambda h)^2}{\lambda^2} \tag{S.237}$$

Using this in (S.223), the power received is

$$P_r = \frac{SG_r\lambda^2}{(4\pi)^2h^2}\Gamma\frac{4\pi(\pi\lambda h)^2}{\lambda^2} \tag{S.238}$$

Simplifying, the radar equation for the passive sounding reflected signal over the Fresnel zone for flat surface, normal incidence and plane wave scattering at the target is

$$P_r = \frac{SG_r\lambda^2\Gamma\pi}{4} \tag{S.239}$$

which predicts a receive power larger than that for spherical wave scattering (previous section) by a factor of $\pi^2/4 \approx 4$ dB. This is exactly analogous to the active case, where the backscatter expression for plane-waves over-predicts the received power compared to the derivation with spherical waves. With no dependence on range, this has also reduced to a 1D scattering problem. This is represented in Figure S31.

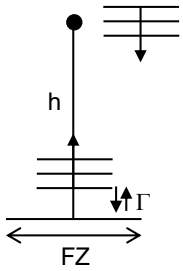

Fig. S31: Passive sounding over flat surface Fresnel zone with normal incidence and plane wave scattering.

S4.4. Passive - Fresnel Zone - Normal Plane Wave Incidence - Spherical Scattering - Spherical Surface

Here we derive the Fresnel zone and radar equation for passive sounding over a spherical surface and normal incidence plane wave using the surface phase integral. The geometry is shown in Figure S32. Let the sensor be aligned with the z-axis. The two-way phase consists of the one-way phase between the sensor and the spherical surface plus the one-way phase from a reference plane of the incident plane wave to the spherical surface. Because the incident wave is planar, a constant offset of the reference plane will not affect the results. Therefore, the plane wave reference plane is chosen to be tangent to the spherical surface at the nadir point. The one-way phase contribution of the incident plane wave is the distance from this reference plane to the spherical surface. The two-way phase integral is given by

$$I = \int_0^{2\pi}\int_0^{\beta} e^{ik(D_1(\theta,\phi)+D_2(\theta,\phi))}r^2\sin\theta d\theta d\phi \tag{S.240}$$

where

$$D_1 = |\mathbf{s} - \mathbf{x}| \tag{S.241}$$

$$\mathbf{s} = (r + h)\hat{z} \tag{S.242}$$

$$\mathbf{x} = r\hat{r} \tag{S.243}$$

$$= r(\sin\theta\cos\phi\hat{x} + \sin\theta\sin\phi\hat{y} + \cos\theta\hat{z}) \tag{S.244}$$

$$D_2 = r - r\cos\theta \tag{S.245}$$

and $\mathbf{s}$ is the vector to the receiver position along the z axis, r is the radius of the sphere, h is the height of the receiver

above the sphere, $\mathbf{x}$ is the integration point on the sphere, D_1 is the distance from the receiver to the integration point, D_2 is the distance from the plane wave reference plane that is tangent to the sphere at nadir to the spherical surface, and β is the integration limit.

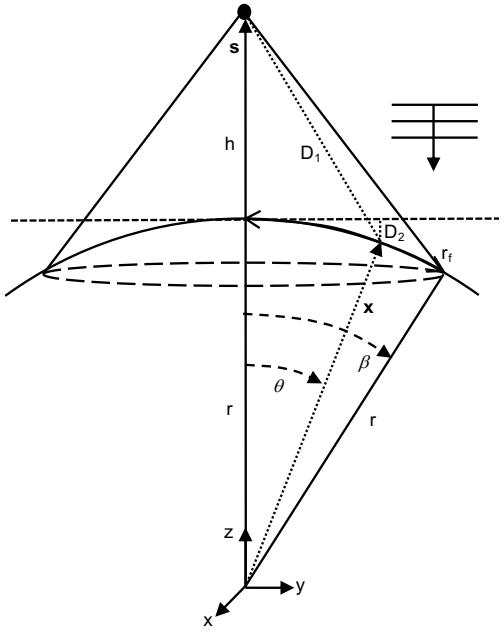

Fig. S32: Passive sounding over a spherical surface Fresnel zone with normal incidence and plane wave scattering.

Similar to the active case, for small integration angles

$$D_1 = \sqrt{r^2 + (r+h)^2 - 2r(r+h)\cos\theta} \quad \text{(S.246)}$$

$$\approx h + \frac{(hr+r^2)}{2h}\theta^2 \quad \text{(S.247)}$$

Also,

$$D_2 \approx r - r(1-\theta^2/2) \quad \text{(S.248)}$$

$$= r\frac{\theta^2}{2} \quad \text{(S.249)}$$

Approximating the differential element as $\sin\theta \approx \theta$, the integral is

$$I \approx 2\pi \int_0^\beta e^{ik(h+\frac{(hr+r^2)}{2h}\theta^2)+ikr\theta^2/2} r^2\theta d\theta \quad \text{(S.250)}$$

$$= 2\pi r^2 e^{ikh} \int_0^\beta e^{iB\theta^2}\theta d\theta \quad \text{(S.251)}$$

$$B = k\left(\frac{hr+r^2}{2h} + \frac{r}{2}\right) \quad \text{(S.252)}$$

$$= \frac{k(2hr+r^2)}{2h} \quad \text{(S.253)}$$

The integral is evaluated as

$$I = 2\pi r^2 \frac{i(e^{i\beta^2 B}-1)}{2B} \quad \text{(S.254)}$$

The magnitude squared is

$$|I|^2 = \left(\frac{2\pi r^2}{2B}\right)^2 \left|e^{i\beta^2 B} - 1\right|^2 \quad \text{(S.255)}$$

This is maximized when

$$\beta^2 B = m\pi \quad \text{(S.256)}$$

For $m = 1$, the integration limit for the first Fresnel zone is

$$\beta = \sqrt{\frac{\pi 2h}{k(2hr+r^2)}} \quad \text{(S.257)}$$

$$= \sqrt{\frac{\lambda}{2}\frac{2h}{2hr+r^2}} \quad \text{(S.258)}$$

The Fresnel zone radius is taken as the arc length along the surface, $r_f = r\beta$, or

$$r_f = \sqrt{\frac{\lambda}{2}\frac{(2h)r}{(2h)+r}} \quad \text{(S.259)}$$

This is the same result as the Fresnel zone for the active case with $h \to 2h$. Again, the sensor appears at twice the height compared to the active sounding case when determining the Fresnel zone radius.

At the Fresnel zone, the magnitude squared of the phase integral is

$$|I|^2 = \frac{4\pi^2}{k^2}\frac{(2h)^2 r^2}{(2h+r)^2} \quad \text{(S.260)}$$

This is same result as for active sounding over a spherical surface except with $h \to 2h$. Using the backscatter for the disk, (S.10),

$$\sigma_{disk} = \Gamma\frac{4\pi|I|^2}{\lambda^2} \quad \text{(S.261)}$$

we get

$$\sigma_{disk} = \Gamma\frac{4\pi}{\lambda^2}\frac{4\pi^2}{k^2}\frac{(2h)^2 r^2}{(2h+r)^2} \quad \text{(S.262)}$$

$$= \Gamma 4\pi\frac{(2h)^2 r^2}{(2h+r)^2} \quad \text{(S.263)}$$

Substituting (S.263) into the passive sounding radar equation for the reflected signal, (S.223), the power received is

$$P_r = \frac{SG_r\lambda^2}{(4\pi)^2 h^2}\Gamma 4\pi\frac{(2h)^2 r^2}{(2h+r)^2} \quad \text{(S.264)}$$

After simplifying, the radar equation for the passive sounding reflected signal of a Fresnel zone over a spherical surface and normal incidence plane wave is

$$P_r = \frac{SG_r\lambda^2\Gamma}{\pi}\frac{r^2}{(2h+r)^2} \quad \text{(S.265)}$$

The geometric factor is the same as that in (Romero-Wolf and others, 2015).

This radar equation should be used when passive sounding is used to investigate a surface and the experiment is conducted in a nadir geometry from an orbiter where the sensor altitude is comparable to the body radius.

S4.5. Passive - Fresnel Zone - Off-nadir Plane Wave Incidence - Spherical Scattering - Flat Surface

Here we derive the Fresnel zone radar equation for the passive sounding receiver over a flat surface with off-nadir wave incidence. The scattering is specular, so the incidence angle is equal to the reflected angle. The incident field on the surface is a plane wave, but we will use the surface phase integral to compute the scattered wave to the receiver over the Fresnel zone. This geometry, represented in Figure S33, is similar to the bi-static geometry for flat surface and spherical waves, Section S5.6.

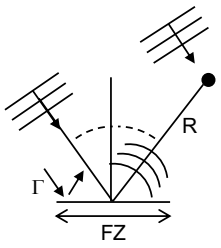

Fig. S33: Representation of passive sounding Fresnel zone with off-nadir incidence.

The Fresnel zone for this geometry is an ellipse with parameters given by (S.296) and (S.297) in the limit when the range of the source or receiver goes to infinity. Let R be the distance from the receiver to the specular point, then the Fresnel zone ellipse parameters are

$$a^2 = \frac{b^2}{\cos^2\theta_i} \tag{S.266}$$

$$b^2 = \lambda R \tag{S.267}$$

The one-way surface phase integral, computed over the Fresnel zone to the receiver, will be the same as (S.330) in Section S5.6 except it will only integrate the vector to the receiver. The result will be (S.352) in the limit that one of the ranges goes to infinity with the other equal to R:

$$|I|^2 = \frac{4\lambda^2}{\cos^2\theta_i} R^2 \tag{S.268}$$

Using this in (S.328), the target cross section in the specular direction is

$$\sigma = \Gamma \frac{4\pi}{\lambda^2} \cos^2\theta_i |I|^2 \tag{S.269}$$

$$= \Gamma 4^2 \pi R^2 \tag{S.270}$$

Substituting this into (S.223), the radar equation for the passive receiver, Fresnel zone, off-nadir incidence, and spherical wave scattering is

$$P_r = \frac{S G_r \lambda^2 \Gamma}{\pi} \tag{S.271}$$

Which is exactly the same as for the normal incidence, Fresnel zone, (S.235). There are two reasons for this. First, because the incident wave is planar and the surface is flat, the incident wave is the same everywhere and so appears to originate from underneath the surface as a plane wave. Second, the area of the Fresnel zone grows with increasing distance to perfectly compensate the range dependence of the scattered field. Therefore, whether the geometry is nadir or off-nadir, the received power is the same and does not depend on range to the target.

S5. BISTATIC

In this section we derive radar equations for general bistatic geometries. These are included for reference and because they provide generalizations for the radar equations and Fresnel zone that reduce to those for the simpler geometries in the previous sections. There are many practical applications of bistatic radar, though most are not in the field of low-frequency radar sounding. Examples include using GPS signals of opportunity for terrestrial remote sensing (Hajj and Zuffada, 2003), or investigating surface scattering of the Moon using a combination of orbiting and ground-based radar systems (Patterson and others, 2017).

S5.1. Bistatic Radar Equation

The bistatic radar equation is, (Ulaby and others, 2014; Hajj and Zuffada, 2003),

$$P_r = \frac{P_t G_t G_r \lambda^2 \sigma}{(4\pi)^3 r_1^2 r_2^2} \tag{S.272}$$

where P_r is the received power, P_t is the transmit power, G_t and G_r are the transmit and receive antenna gains respectively, r_1 is the distance to the target from the transmitter, and r_2 is the distance to the target from the receiver. See Figure S34. G_t, G_r, and σ are functions of incident direction, scattering direction, and polarization. Simply put, this is the same as the basic radar equation, (S.1), with the R^4 geometric spreading split so that one factor of R^2 applies to the source and one factor applies to the receiver.

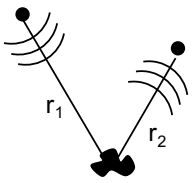

Fig. S34: Geometry for the general bistatic radar equation.

Derivation

The power density of the signal from the transmitter is

$$S_t = \frac{P_t G_t}{4\pi r_1^2} \tag{S.273}$$

The power intercepted by the target is $P_i = S_t \sigma$. This is reradiated from the target to the receiver with power density

$$S_r = \frac{P_i}{4\pi r_2^2} \tag{S.274}$$

The power intercepted by the receive antenna is

$$P_r = S_r A_r \tag{S.275}$$

Putting these together gives (S.272).

S5.2. Bistatic - Image Method - Spherical Waves - Flat Surface

Here we derive the bistatic radar equation over a flat surface using the image method. Similar to S1.2, the half-space is replaced with an image source reflected over the interface. The geometry is shown in Figure S35. Let r_1 and r_2 be the distances from the source and receiver to the specular point. The power density at the receiver due to the image source is

$$S_r = \frac{P_t G_t}{4\pi(r_1 + r_2)^2} \tag{S.276}$$

The power received is then

$$P_r = S_r A_r \tag{S.277}$$

where A_r is the effective aperture of the receiver. After including a factor of reflectivity, Γ, the power received is

$$P_r = \frac{P_t G_t G_r \lambda^2 \Gamma}{(4\pi)^2 (r_1 + r_2)^2} \tag{S.278}$$

This appears in (Ulaby and others, 2014; Carreno-Luengo and others, 2018). When $r_1 = r_2 = h$, (S.278) reduces to the radar equation for the image method at normal incidence, (S.9).

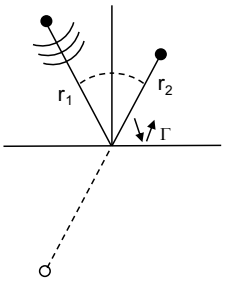

Fig. S35: Geometry for the bistatic radar equation under the image method.

S5.3. Bistatic Fresnel Zone Ellipse - Flat Surface

The bistatic Fresnel zone is the region over which the phase between a source and receiver in a specular geometry has changed less than $\lambda/2$. Specular geometry implies 1) the incident and scattered angles are equal (Snell's law), 2) the source and receiver lie in a plane, 3) the source and receiver are allowed to be at different distances. The bistatic Fresnel zone is derived by solving for the contour that describes the boundary of the Fresnel zone over a flat surface.

The geometry is shown in Figure S36. The surface is the XY plane, the specular point is the origin, and the source and receiver lie in the XZ plane at locations

$$\mathbf{r}_1 = r_1 (\sin\theta_i \hat{x} + \cos\theta_i \hat{z}) \tag{S.279}$$

$$\mathbf{r}_2 = r_2 (-\sin\theta_i \hat{x} + \cos\theta_i \hat{z}) \tag{S.280}$$

where θ_i is the incidence angle measured from the z axis. A point in the plane is given generally as

$$\mathbf{x} = x\hat{x} + y\hat{y} \tag{S.281}$$

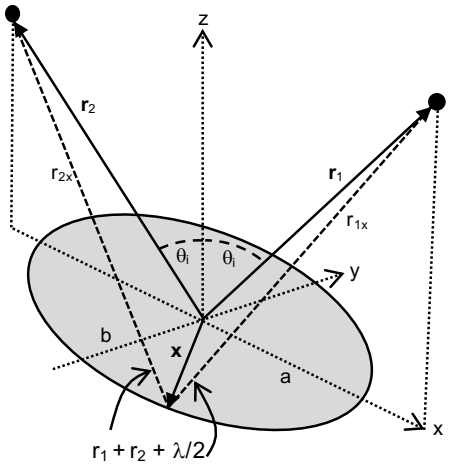

Fig. S36: Geometry for the bistatic Fresnel zone ellipse for a flat surface.

The total distance measured between the source and receiver relative to the origin is $t_1 = r_1 + r_2$. While the distance between the source and receiver through a point in the plane is $t_2 = r_{1x} + r_{2x}$. The Fresnel condition is

$$t_2 - t_1 = \lambda/2 \tag{S.282}$$

where this is the difference in the total paths of the specular point and any point in the plane. Substituting

$$r_{1x} + r_{2x} - (r_1 + r_2) = \lambda/2 \tag{S.283}$$

The magnitude of the vector from the source to a point in the plane is

$$r_{1x} = |\mathbf{r}_1 - \mathbf{x}| \tag{S.284}$$

$$= \left[(r_1 \sin\theta_i - x)^2 + y^2 + r_1^2 \cos^2\theta_i\right]^{1/2} \tag{S.285}$$

$$= \left[r_1^2 \sin^2\theta_i - 2r_1 x \sin\theta_i + x^2 + y^2 + r_1^2 \cos^2\theta_i\right]^{1/2} \tag{S.286}$$

$$= \left[r_1^2 - 2r_1 x \sin\theta_i + x^2 + y^2\right]^{1/2} \tag{S.287}$$

Likewise for the receiver

$$r_{2x} = |\mathbf{r}_2 - \mathbf{x}| \tag{S.288}$$

$$= \left[(-r_2 \sin\theta_i - x)^2 + y^2 + r_2^2 \cos^2\theta_i\right]^{1/2} \tag{S.289}$$

$$= \left[r_2^2 + 2r_2 x \sin\theta_i + x^2 + y^2\right]^{1/2} \tag{S.290}$$

Assuming r_1 and r_2 are large compared to the coordinates x and y, the square root in (S.287) and (S.290) is approximated with

$$\left[1 + A/w + B/w^2\right]^{1/2} \approx 1 + \frac{A}{2w} + \frac{4B - A^2}{8w^2} + \ldots \tag{S.291}$$

which is kept to second order to preserve x^2 and y^2. Then

$$r_{1x} \approx r_1 - x\sin\theta_i + \frac{x^2(1 - \sin^2\theta_i) + y^2}{2r_1} \tag{S.292}$$

$$r_{2x} \approx r_2 + x\sin\theta_i + \frac{x^2(1 - \sin^2\theta_i) + y^2}{2r_2} \tag{S.293}$$

Substituting these into (S.283), the radial and linear terms cancel giving the following equation

$$\frac{x^2\cos^2\theta_i + y^2}{2r_1} + \frac{x^2\cos^2\theta_i + y^2}{2r_2} = \frac{\lambda}{2} \tag{S.294}$$

This is an ellipse

$$\frac{x^2}{a^2} + \frac{y^2}{b^2} = 1 \tag{S.295}$$

with parameters

$$a^2 = \frac{b^2}{\cos^2\theta_i} \tag{S.296}$$

$$b^2 = \frac{\lambda r_1 r_2}{r_1 + r_2} \tag{S.297}$$

This ellipse approximates the Fresnel zone boundary. Note $a \geq b$ so the ellipse is oriented lengthwise between the source and receiver. Equations (S.296) and (S.297) are equivalent to the ellipse parameters given in (Hajj and Zuffada, 2003). The eccentricity is

$$e = \sqrt{1 - \frac{b^2}{a^2}} \tag{S.298}$$

$$= \sqrt{1 - \cos^2\theta_i} \tag{S.299}$$

$$= \sin\theta_i \tag{S.300}$$

The area of an ellipse is $A = \pi ab$, therefore the area of the bistatic Fresnel zone is

$$A = \frac{\pi}{\cos\theta_i}\frac{\lambda r_1 r_2}{r_1 + r_2} \tag{S.301}$$

For normal incidence, $\theta_i = 0$, the boundary is a circle and the Fresnel zone radius for two sensors at different altitudes at nadir over a flat surface is

$$r_f = \sqrt{\frac{\lambda h_1 h_2}{h_1 + h_2}} \tag{S.302}$$

This appears in (Schroeder and others, 2016). When $h_1 = h_2 = h$ this becomes the usual $r_f = \sqrt{\lambda h/2}$.

S5.4. Bistatic Fresnel Zone Ellipse - Spherical Surface

Here we derive a curve that approximates the boundary of the Fresnel zone over a spherical surface having radius r. The geometry is shown in Figure S37. As before, the source and receiver lie in the XZ plane. The origin is the specular point on the surface of the sphere, where the sphere is centered at $z = -r$. The source and receiver are at locations

$$\mathbf{r}_1 = r_1\sin\theta_i\hat{x} + r_1\cos\theta_i\hat{z} \tag{S.303}$$

$$\mathbf{r}_2 = -r_2\sin\theta_i\hat{x} + r_2\cos\theta_i\hat{z} \tag{S.304}$$

where θ_i is the incidence angle measured from the z axis. A point on the sphere satisfies

$$x^2 + y^2 + (z + r)^2 = r^2 \tag{S.305}$$

so that the vector from the origin to a point on the upper half of the sphere can be written

$$\mathbf{x} = x\hat{x} + y\hat{y} + z\hat{z} \tag{S.306}$$

$$= x\hat{x} + y\hat{y} + (\sqrt{r^2 - x^2 - y^2} - r)\hat{z} \tag{S.307}$$

As with the flat surface, the total distance measured between the source and receiver relative to the specular point is $t_1 = r_1 + r_2$. While the distance between the source and receiver through a point on the sphere is $t_2 = r_{1s} + r_{2s}$. The Fresnel condition is again

$$t_2 - t_1 = \lambda/2 \tag{S.308}$$

where the two-way difference in distance is $\lambda/2$ between the specular point and the Fresnel boundary. Substituting

$$r_{1s} + r_{2s} - (r_1 + r_2) = \lambda/2 \tag{S.309}$$

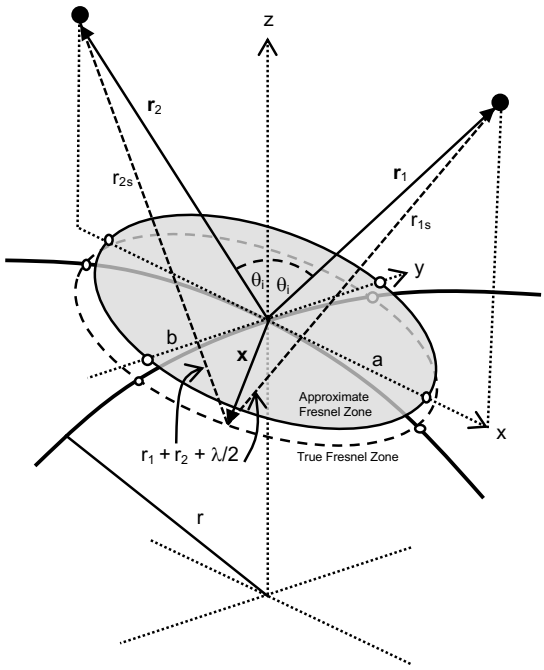

Fig. S37: Geometry for the bistatic Fresnel zone ellipse over a spherical surface. The ellipse is a planar approximation of the actual Fresnel zone over the sphere.

The magnitude of the vector from the source to the sphere is

$$r_{1s} = |\mathbf{r}_1 - \mathbf{x}| \tag{S.310}$$

$$= \Big[(r_1\sin\theta_i - x)^2 + y^2 + (r_1\cos\theta_i + r - \sqrt{r^2 - x^2 - y^2})^2\Big]^{1/2} \tag{S.311}$$

$$= \Big[r_1^2 - 2r_1 x\sin\theta_i + 2r_1 r\cos\theta_i - 2r_1\cos\theta_i\sqrt{r^2 - x^2 - y^2} + 2r^2 - 2r\sqrt{r^2 - x^2 - y^2}\Big]^{1/2} \tag{S.312}$$

Assuming $r \gg x, y$, the square roots are expanded as $\sqrt{1-x} = 1 - x/2 + ...$, which simplifies to

$$r_{1s} \approx \Big[r_1^2 - 2r_1 x\sin\theta_i + (1 + \frac{r_1}{r}\cos\theta_i)(x^2 + y^2)\Big]^{1/2} \tag{S.313}$$

which is the same for r_{2s} with + on the linear term. Assuming that r_1 and r_2 are large compared to the coordinates x and y, and using (S.291),

$$r_{1s} = r_1 \left[1 - \frac{2x\sin\theta_i}{r_1} + \frac{1}{r_1^2}(1 + \frac{r_1}{r}\cos\theta_i)(x^2+y^2)\right]^{1/2} \tag{S.314}$$

$$\approx r_1 - x\sin\theta_i + \frac{(1+\frac{r_1}{r}\cos\theta_i)(x^2+y^2) - x^2\sin^2\theta_i}{2r_1} \tag{S.315}$$

Likewise for r_{2s} except + on the linear term:

$$r_{2s} \approx r_1 + x\sin\theta_i + \frac{(1+\frac{r_1}{r}\cos\theta_i)(x^2+y^2) - x^2\sin^2\theta_i}{2r_1} \tag{S.316}$$

Substituting into the Fresnel condition, (S.309), the radial and linear terms cancel giving the following equation

$$\frac{(1+\frac{r_1}{r}\cos\theta_i)(x^2+y^2) - x^2\sin^2\theta_i}{2r_1} + \frac{(1+\frac{r_2}{r}\cos\theta_i)(x^2+y^2) - x^2\sin^2\theta_i}{2r_2} = \frac{\lambda}{2} \tag{S.317}$$

Rearranged as the equation for an ellipse

$$\frac{x^2}{a^2} + \frac{y^2}{b^2} = 1 \tag{S.318}$$

with parameters

$$a^2 = \left[\frac{r_1+r_2}{\lambda r_1 r_2}\cos^2\theta_i + \frac{2}{\lambda r}\cos\theta_i\right]^{-1} \tag{S.319}$$

$$b^2 = \left[\frac{r_1+r_2}{\lambda r_1 r_2} + \frac{2}{\lambda r}\cos\theta_i\right]^{-1} \tag{S.320}$$

This ellipse approximates the Fresnel zone boundary. It is not the actual shape of the Fresnel zone contour, because a planar cut through the sphere must be a circle. Instead, this is a slightly smaller ellipse compared to the flat surface case which approximates the Fresnel contour on the sphere. In addition, the approximation will be progressively worse for wider incidence angles (e.g., grazing), when the x and y extents of the Fresnel zone become large fractions of the body radius and violate the conditions of the expansions above.

The ellipse is still oriented with its semi-major axis in the plane of the source and receiver. The eccentricity is

$$e = \sqrt{1 - \frac{b^2}{a^2}} \tag{S.321}$$

$$= \sin\theta_i \left[1 + \frac{r_1 r_2}{r_1+r_2}\frac{2}{r}\cos\theta_i\right]^{-1/2} \tag{S.322}$$

which shows that the Fresnel zone is slightly smaller than that for a flat surface, (S.300).

Note, the Fresnel zone for every surface geometry (e.g., monostatic/bistatic, active/passive, flat/curved surfaces) can be derived from (S.319) and (S.320) with appropriate limits. For example, for two sensors at normal incidence, $\theta_i = 0$, and different altitudes, $r_1 = h_1$, $r_2 = h_2$, over a spherical surface the boundary is a circle with

$$a^2 = b^2 = \left[\frac{h_1+h_2}{\lambda h_1 h_2} + \frac{2}{\lambda r}\right]^{-1} \tag{S.323}$$

$$= \frac{\lambda r h_1 h_2}{r(h_1+h_2) + 2h_1 h_2} \tag{S.324}$$

$$\tag{S.325}$$

Then the Fresnel zone radius is

$$r_f = \sqrt{\frac{\lambda r h_1 h_2}{r(h_1+h_2) + 2h_1 h_2}} \tag{S.326}$$

This reduces to the usual expression for the Fresnel zone radius over a spherical surface when $h_1 = h_2 = h$,

$$r_f = \sqrt{\frac{\lambda r h}{2(r+h)}} \tag{S.327}$$

S5.5. Target Specular Scatter

The radar cross section for specular scattering under the Kirchhoff approximation is

$$\sigma = \Gamma \frac{4\pi}{\lambda^2}\cos^2\theta_i |I|^2 \tag{S.328}$$

where θ_i is the incident and reflected angle, Γ is the reflectivity evaluated at θ_i, and $|I|^2$ is the magnitude squared of the surface phase integral for spherical incident waves. The reflectivity is also polarization dependent.

For plane wave incidence and specular scattering, the magnitude squared of the surface phase integral reduces to the area squared:

$$\sigma = \Gamma \frac{4\pi}{\lambda^2}\cos^2\theta_i A^2 \tag{S.329}$$

S5.6. Bistatic - Fresnel Zone - Spherical Waves - Flat Surface

Here we derive the radar equation for bistatic scattering from the Fresnel zone for a spherical wave incidence on a flat surface. This is represented in Figure S38. The geometry and variables are the same as those given in S5.3. Even though we derived the Fresnel zone previously, starting from the surface phase integral allows us to 1) confirm the previous result, 2) derive the correct multiplying constants in the radar equation.

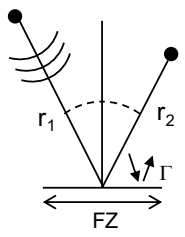

Fig. S38: Bistatic Fresnel zone with spherical wave incidence.

The geometry is shown in Figure S39. The surface phase integral is

$$I = \int e^{ik(r_{1x}+r_{2x})} dS \tag{S.330}$$

where r_{1x} and r_{2x} are the distances from the source and receiver to a point on the flat surface. Using the large argument approximations for the distance between the source/surface and receiver/surface, (S.292) and (S.293), the sum in the exponent is

$$r_{1x} + r_{2x} \approx r_1 + r_2 + \frac{x^2 \cos^2\theta_i + y^2}{2r_1} + \frac{x^2 \cos^2\theta_i + y^2}{2r_2} \tag{S.331}$$

$$= r_1 + r_2 + x^2 \cos^2\theta_i \frac{r_1 + r_2}{2r_1 r_2} + y^2 \frac{r_1 + r_2}{2r_1 r_2} \tag{S.332}$$

where r_1 and r_2 are the distances from the source and receiver to the center of the Fresnel zone.

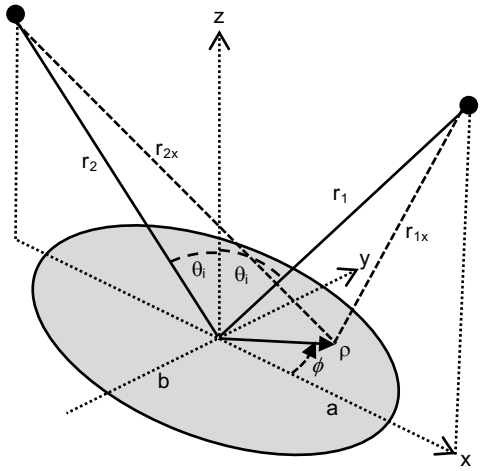

Fig. S39: Geometry for the bistatic Fresnel zone ellipse with spherical wave incidence.

Assuming the area to be an ellipse,

$$\frac{x^2}{a^2} + \frac{y^2}{b^2} = 1 \tag{S.333}$$

the integral is parameterized as

$$x = a\rho\cos\phi \tag{S.334}$$

$$y = b\rho\sin\phi \tag{S.335}$$

with surface element $dS = ab\rho d\rho d\phi$, so that

$$I = \int_0^{2\pi}\int_0^1 e^{ik(r_{1x}+r_{2x})} ab\rho d\rho d\phi \tag{S.336}$$

Substituting

$$r_{1x} + r_{2x} \approx r_1 + r_2 + a^2\rho^2\cos^2\phi\cos^2\theta_i \frac{r_1 + r_2}{2r_1 r_2} + b^2\rho^2\sin^2\phi \frac{r_1 + r_2}{2r_1 r_2} \tag{S.337}$$

The integral can then be written

$$I = abe^{ik(r_1+r_2)} \int_0^{2\pi}\int_0^1 e^{i(A\rho^2\cos^2\phi + B\rho^2\sin^2\phi)} \rho d\rho d\phi \tag{S.338}$$

where

$$A = ka^2\cos^2\theta_i \frac{r_1 + r_2}{2r_1 r_2} \tag{S.339}$$

$$B = kb^2 \frac{r_1 + r_2}{2r_1 r_2} \tag{S.340}$$

Using the identity:

$$\int_0^{2\pi} e^{u\cos^2\phi + v\sin^2\phi} d\phi = 2\pi e^{(u+v)/2} I_0\left(\frac{u-v}{2}\right) \tag{S.341}$$

(S.338) becomes

$$I = 2\pi abe^{ik(r_1+r_2)} \int_0^1 e^{i\rho^2(A+B)/2} I_0\left(\frac{i\rho^2(A-B)}{2}\right)\rho d\rho \tag{S.342}$$

which does not have a solution. To continue, if $r_1 \gg 1$ and $r_2 \gg 1$, the argument of the Bessel function is small. Using $I_0(x \to 0) \approx 1$, the integral is approximated as

$$I \approx 2\pi abe^{ik(r_1+r_2)} \int_0^1 e^{i\rho^2(A+B)/2} \rho d\rho \tag{S.343}$$

Using

$$\int_0^1 e^{icx^2} x dx = \frac{i(1 - e^{ic})}{2c} \tag{S.344}$$

(S.343) is evaluated as

$$I = 2\pi abe^{ik(r_1+r_2)} \frac{i\left(1 - e^{i(A+B)/2}\right)}{A+B} \tag{S.345}$$

The magnitude is

$$|I| = \frac{2\pi ab}{A+B}\left|1 - e^{i(A+B)/2}\right| \tag{S.346}$$

The magnitude is maximized when

$$\frac{A+B}{2} = m\pi \tag{S.347}$$

For $m = 1$, we have

$$ka^2\cos^2\theta_i \frac{r_1 + r_2}{4r_1 r_2} + kb^2 \frac{r_1 + r_2}{4r_1 r_2} = \pi \tag{S.348}$$

Which is satisfied for ellipse parameters

$$a^2 = \frac{b^2}{\cos^2\theta_i} \tag{S.349}$$

$$b^2 = \frac{\lambda r_1 r_2}{r_1 + r_2} \tag{S.350}$$

which are the same as (S.296) and (S.297). Using these in (S.346), the magnitude squared of the surface phase integral is

$$|I|^2 = \frac{4^2\pi^2 a^2 b^2}{(A+B)^2} \tag{S.351}$$

$$= \frac{4}{\cos^2\theta_i} \frac{\lambda^2 r_1^2 r_2^2}{(r_1 + r_2)^2} \tag{S.352}$$

Using this in (S.328), the target cross section in the specular direction is

$$\sigma = \Gamma \frac{4\pi}{\lambda^2} \cos^2\theta_i |I|^2 \tag{S.353}$$

$$= \Gamma 4^2 \pi \frac{r_1^2 r_2^2}{(r_1+r_2)^2} \tag{S.354}$$

Substituting this into (S.272), the radar equation for bistatic geometry, Fresnel zone, spherical waves, and flat interface is

$$P_r = \frac{P_t G_t G_r \lambda^2 \Gamma}{4\pi^2 (r_1+r_2)^2} \tag{S.355}$$

When the source and receiver are collocated at $r_1 = r_2 = h$, this reduces to (S.28). This is the same as (S.278) except for a difference of a factor of 4 in the denominator, which, like its normal-incidence counterparts, this difference comes from the integration of spherical waves over the Fresnel zone instead of assuming plane waves incidence at the target.

S5.7. Bistatic - Fresnel Zone - Plane Waves - Flat Surface

For a bistatic geometry over a flat surface, the Fresnel zone is an ellipse with area $A = \pi ab$ having parameters (S.296) and (S.297). Assuming plane wave incidence at the surface, then using these in (S.329), the scattering cross section in the specular direction is

$$\sigma = \Gamma \frac{4\pi}{\lambda^2} \cos^2\theta_i (\pi ab)^2 \tag{S.356}$$

$$= \Gamma 4\pi^3 \left(\frac{r_1 r_2}{r_1+r_2} \right)^2 \tag{S.357}$$

Using this in (S.272), the radar equation for specular bistatic geometry, Fresnel zone, flat surface, and plane wave incidence is

$$P_r = \frac{P_t G_t G_r \lambda^2 \Gamma}{4^2 (r_1+r_2)^2} \tag{S.358}$$

This is represented in Figure S40. When the source and receiver are co-located above the surface at a distance $r_1 = r_2 = h$, then (S.358) reduces to the radar equation from the 'antenna' approach, Section S1.6, (S.60).

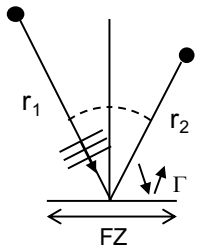

Fig. S40: Geometry for the bistatic Fresnel zone area with plane wave incidence.

S5.8. Bistatic - Fresnel Zone - Spherical Waves - Spherical Surface

The derivation for the radar equation for the bistatic Fresnel zone over a spherical surface using the surface phase integral for spherical wave incidence follows that for the flat surface in Section S5.6. We already have an expression for the bistatic Fresnel zone ellipse for spherical surface under large argument approximations derived in Section S5.4. We will make use of both sections. As before, the purpose of using the surface phase integral is derive the correct multiplying constants in the radar equation.

The geometry is shown in Figure S41. The surface phase integral is

$$I = \int e^{ik(r_{1s}+r_{2s})} dS \tag{S.359}$$

where r_{1s} and r_{2s} are the distances from the source and receiver to the spherical surface as described in Section S5.4. When the radius of the sphere is large compared to the size of the Fresnel zone, the sum in the exponent is approximated as

$$r_{1s}+r_{2s} \approx r_1+r_2 + \frac{(1+\frac{r_1}{r}\cos\theta_i)(x^2+y^2) - x^2\sin^2\theta_i}{2r_1} + \frac{(1+\frac{r_2}{r}\cos\theta_i)(x^2+y^2) - x^2\sin^2\theta_i}{2r_2} \tag{S.360}$$

$$= r_1+r_2 + \left(\frac{r_1+r_2}{2r_1r_2}\cos^2\theta_i + \frac{\cos\theta_i}{r} \right) x^2 + \left(\frac{r_1+r_2}{2r_1r_2} + \frac{\cos\theta_i}{r} \right) y^2 \tag{S.361}$$

The contour of the bistatic Freznel zone on the sphere is neither a circle, nor a true ellipse, but a saddle, with the lowest points of the contour lying in the plane of the source and receiver. Formally maximizing (S.359) should reveal this contour exactly. Instead, we want to arrive at the planar ellipse derived in Section S5.4 that approximates this contour. This is to 1) simplify the derivation, and 2) ensure that we get the same elliptical boundary as in Section S5.4 while also giving us the corresponding multiplying constants for the Fresnel zone target in the radar equation. To accomplish this, we will evaluate the surface phase integral over the domain of an ellipse. The ellipse lies in a plane perpendicular to the normal direction at the specular point. We then find the parameters of the ellipse that maximize the surface phase integral, taking care to evaluate and approximate the differential surface element under this mapping.

In general, a surface integral parameterized by two variables is written

$$\iint f dS = \iint f(\mathbf{x}(u,v)) \left\| \frac{\partial \mathbf{x}}{\partial u} \times \frac{\partial \mathbf{x}}{\partial v} \right\| du dv \tag{S.362}$$

where u and v range over the planar domain of integration. Let a point on the sphere centered at $z = -r$ be

$$\mathbf{x} = \begin{bmatrix} x \\ y \\ z = \sqrt{r^2 - x^2 - y^2} - r \end{bmatrix} \tag{S.363}$$

The domain of integration is an ellipse in the XY plane and parameterized as

$$x = a\rho\cos\phi \tag{S.364}$$
$$y = b\rho\sin\phi \tag{S.365}$$

where $\rho = [0,1]$ and $\phi = [0, 2\pi]$, with a and b to be solved for. The integration domain is shown in Figure S41 (shifted for display). Substituting (S.364) and (S.365) into (S.363) and assuming r is large

$$\mathbf{x} \approx \begin{bmatrix} a\rho\cos\phi \\ b\rho\sin\phi \\ \dfrac{-a^2\rho^2\cos^2\phi - b^2\rho^2\sin^2\phi}{2r} \end{bmatrix} \tag{S.366}$$

Using this with $(u, v) = (\rho, \phi)$, the cross product norm is evaluated as

$$\left\| \frac{\partial \mathbf{x}}{\partial \rho} \times \frac{\partial \mathbf{x}}{\partial \phi} \right\| \approx \left[\frac{a^2b^2\rho^2(a^2\rho^2\cos^2\phi + b^2\rho^2\sin^2\phi + r^2)}{r^2} \right]^{1/2} \tag{S.367}$$

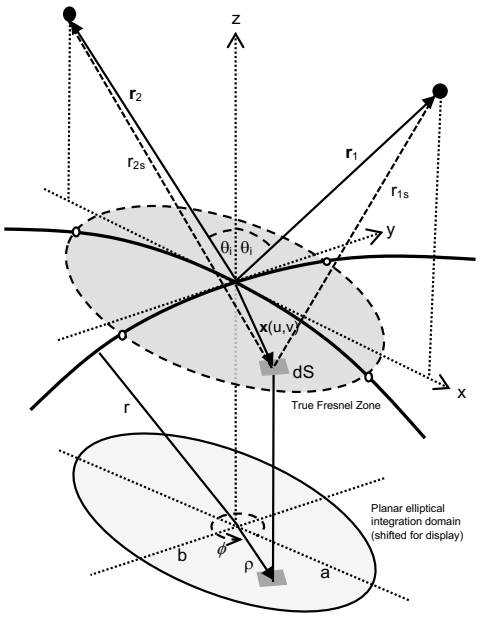

Fig. S41: Geometry for the bistatic Fresnel zone ellipse with spherical wave incidence.

Assuming $r \gg a, b, \rho$, this is approximated

$$\left\| \frac{\partial \mathbf{x}}{\partial \rho} \times \frac{\partial \mathbf{x}}{\partial \phi} \right\| \approx ab\rho \tag{S.368}$$

which is simply the scale factor for the differential surface element of an ellipse. The purpose of this was to show that two approximations were needed to simplify the integral: 1) the large argument approximation for the integration point on the sphere, 2) the large argument approximation for the differential surface element.

Substituting (S.364) and (S.365) into (S.361), using (S.368), and using the ellipse parameterization and its limits, the surface phase integral (S.359) can be written

$$I = abe^{ik(r_1+r_2)} \int_0^{2\pi} \int_0^1 e^{i(A\rho^2\cos^2\phi + B\rho^2\sin^2\phi)} \rho d\rho d\phi \tag{S.369}$$

where

$$A = ka^2 \left(\frac{r_1 + r_2}{2r_1r_2}\cos^2\theta_i + \frac{\cos\theta_i}{r} \right) \tag{S.370}$$
$$B = kb^2 \left(\frac{r_1 + r_2}{2r_1r_2} + \frac{\cos\theta_i}{r} \right) \tag{S.371}$$

This is exactly the same as (S.338) only with different constants in the exponent. Therefore, following Section S5.6, the ellipse parameters that maximize the magnitude of the surface phase integral are

$$a^2 = \left[\frac{r_1 + r_2}{\lambda r_1 r_2}\cos^2\theta_i + \frac{2}{\lambda r}\cos\theta_i \right]^{-1} \tag{S.372}$$
$$b^2 = \left[\frac{r_1 + r_2}{\lambda r_1 r_2} + \frac{2}{\lambda r}\cos\theta_i \right]^{-1} \tag{S.373}$$

which are just (S.319) and (S.320), Section S5.4. The magnitude squared is likewise given by (S.351):

$$|I|^2 = \frac{4^2\pi^2a^2b^2}{(A+B)^2} \tag{S.374}$$
$$= 4a^2b^2 \tag{S.375}$$

Using (S.375) in (S.328), the target cross section in the specular direction is

$$\sigma = \Gamma\frac{4^2\pi}{\lambda^2}\cos^2\theta_i a^2b^2 \tag{S.376}$$

Substituting (S.376) into the general bistatic radar equation, (S.272), the radar equation for specular bistatic geometry, Fresnel zone, spherical waves, and spherical surface is

$$P_r = \frac{P_tG_tG_r\Gamma}{4\pi^2r_1^2r_2^2}a^2b^2\cos^2\theta_i \tag{S.377}$$

where a^2 and b^2 are given by (S.319) and (S.320). Written out, this is

$$P_r = \frac{P_tG_tG_r\lambda^2\Gamma}{4\pi^2r_1^2r_2^2}\left[\frac{r_1 + r_2}{r_1r_2}\cos^2\theta_i + \frac{2}{r}\cos\theta_i \right]^{-1} \cdot \left[\frac{r_1 + r_2}{r_1r_2} + \frac{2}{r}\cos\theta_i \right]^{-1} \cos^2\theta_i \tag{S.378}$$

The radar equation for every surface Fresnel zone geometry can be derived from (S.378) with appropriate limits. For example, when $r \to \infty$, this reduces to the radar equation for specular bistatic geometry over a flat surface, (S.355), when $\theta_i = 0$ and $r_1 = r_2 = h$ this reduces to the radar equation for normal incidence over a spherical surface, (S.56), and so on.

S5.9. Bistatic Radar Equation - Subsurface Receiver - Flat Surface

Here we derive the radar equation for a receiver in the subsurface. This is the subsurface analogue of the Friis transmission formula. This applies to experiments or simulations with imbedded or submerged sensors. See Figure S42.

Following Section S2.4, we start with the power density of the image source in the subsurface medium, (S.105), repeated here

$$S' = \frac{P_t G_t T}{4\pi(r_1' + r_2)^2} \frac{r_1'^2}{r_1^2} \frac{\cos\theta_i}{\cos\theta_t} \tag{S.379}$$

The power received by the subsurface receiver is

$$P_r = S' A_r = \frac{S' G_r \lambda_{\epsilon_r}^2}{4\pi} \tag{S.380}$$

where A_r is the effective aperture of the receiver in the subsurface medium, and G_r and λ_{ϵ_r} are the receiver gain and wavelength in the medium. Substituting (S.379) into (S.380), then using (S.120) as well as Snell's law, the power received by the receiver in the subsurface is

$$P_r = \frac{P_t G_t G_r \lambda^2 T}{(4\pi)^2 (r_1 + r_2)^2} \frac{g_r'^2}{n^2} \frac{\cos\theta_i}{\cos\theta_t} \tag{S.381}$$

where g_r' is the off-nadir refraction gain (S.125). Equation (S.381) contains both refraction gain and an area projection term for power propagating through the surface interface. The factor of $1/n^2$ can be thought of as belonging with λ^2 which comes from the effective aperture of the receiver in the medium.

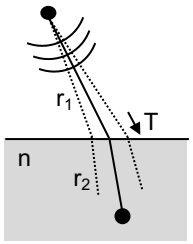

Fig. S42: Geometry for the bistatic radar equation for a subsurface receiver.